1990

Development of a high performance liquid chromatographic method for the determination of the kinetic mechanism of arginine specific ADP-ribosyl transferases

Jacqueline Sue-Anhalt Larew
Iowa State University

INFORMATION TO USERS

The most advanced technology has been used to photograph and reproduce this manuscript from the microfilm master. UMI films the text directly from the original or copy submitted. Thus, some thesis and dissertation copies are in typewriter face, while others may be from any type of computer printer.

The quality of this reproduction is dependent upon the quality of the copy submitted. Broken or indistinct print, colored or poor quality illustrations and photographs, print bleedthrough, substandard margins, and improper alignment can adversely affect reproduction.

In the unlikely event that the author did not send UMI a complete manuscript and there are missing pages, these will be noted. Also, if unauthorized copyright material had to be removed, a note will indicate the deletion.

Oversize materials (e.g., maps, drawings, charts) are reproduced by sectioning the original, beginning at the upper left-hand corner and continuing from left to right in equal sections with small overlaps. Each original is also photographed in one exposure and is included in reduced form at the back of the book.

Photographs included in the original manuscript have been reproduced xerographically in this copy. Higher quality 6" x 9" black and white photographic prints are available for any photographs or illustrations appearing in this copy for an additional charge. Contact UMI directly to order.

U·M·I

University Microfilms International
A Bell & Howell Information Company
300 North Zeeb Road, Ann Arbor, MI 48106-1346 USA
313/761-4700 800/521-0600

Order Number 9035090

Development of a high-performance liquid chromatographic method for the determination of the kinetic mechanism of arginine-specific ADP-ribosyl transferases

Larew, Jacqueline Sue-Anhalt, Ph.D.

Iowa State University, 1990

U·M·I
300 N. Zeeb Rd.
Ann Arbor, MI 48106

Development of a high performance liquid chromatographic method for the determination of the kinetic mechanism of arginine specific ADP-ribosyl transferases

by

Jacqueline Sue-Anhalt Larew

A Dissertation Submitted to the
Graduate Faculty in Partial Fulfillment of the
Requirements for the Degree of
DOCTOR OF PHILOSOPHY

Department: Chemistry
Major: Analytical Chemistry

Approved:

Signature was redacted for privacy.
In Charge of Major Work

Signature was redacted for privacy.
For the Major Department

Signature was redacted for privacy.
For the Graduate College

Iowa State University
Ames, Iowa

1990

TABLE OF CONTENTS

LIST OF FIGURES

LIST OF TABLES

DEDICATION

This work is dedicated to

my parents.

SYMBOLS AND ABBREVIATIONS

3-ABA	3-aminobenzamide
ADP	adenosine diphosphate
ATP	adenosine triphosphate
cAMP	3',5'-cyclic adenosine monophosphate
Con A	concanavalin A
DEA-BAG	diethylamino benzylidine aminoguanidine
DI	deionized
DNA	deoxyribonucleic acid
DTT	dithiothreitol
G_i	inhibitory subunit of a GTP-binding protein
G_s	stimulatory subunit of a GTP-binding protein
GTP	guanine triphosphate
HPLC	high performance liquid chromatography
K_I	inhibition equilibrium constant
K_m	Michaelis constant
LAME	L-arginine methyl ester
NAD	nicotinamide adenine dinucleotide (oxidized form)
NADH	nicotinamide adenine dinucleotide (reduced form)
OPA	ortho-phthaldialdehyde
TCA	trichloroacetic acid
THF	tetrahydrofuran
UV	ultraviolet
V_{max}	maximal velocity

I. INTRODUCTION

A. Review of ADP-ribosylation

The role of posttranslational modification of proteins in the regulation of biological processes has been extensively studied. Some of the modifications most thoroughly studied include acetylation, methylation, and phosphorylation. ADP-ribosylation is another type of covalent modification whose role in the regulation of cellular metabolism is yet to be understood.

ADP-ribosylation involves the transfer of an ADP-ribose group from NAD to an acceptor protein (Figure 1). There are two types of ADP-ribosylation reactions that may occur within a cell. The first type, known as poly-ADP-ribosylation, occurs primarily in the nucleus (1). Poly-ADP-ribose synthetase (EC-2.4.2.30) is responsible for the transfer of a series of ADP-ribose units to histones and other nuclear proteins resulting in a polymeric chain of ADP-ribose units (2). The existence of a poly-ADP-ribose glycohydrolase enzyme (3,4), along with reports of increased ADP-ribosyl transferase activity during cell proliferation (5), differentiation (6-9), transformation (10) and DNA repair (11-14) supports the role of poly-ADP-ribosylation as a regulator of cellular metabolism.

The second type of ADP-ribosylation reaction involves the transfer of a single ADP-ribose unit to an acceptor protein and is therefore known as mono-ADP-ribosylation. Mono-ADP-ribosylation has been reported in a wide variety of cellular systems. Bacterial toxins such as cholera toxin

Figure 1. ADP-ribosylation reaction scheme with LAME as the acceptor

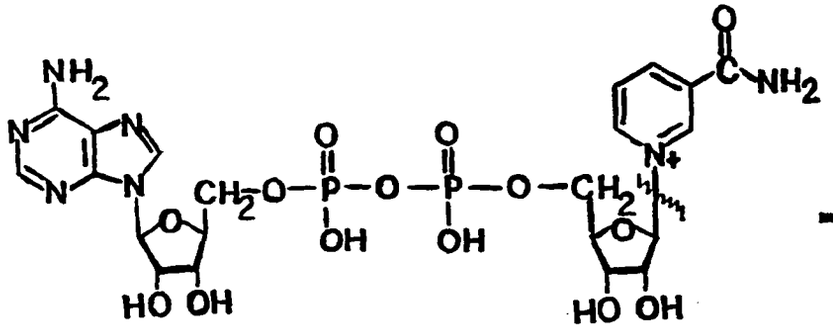

NAD+

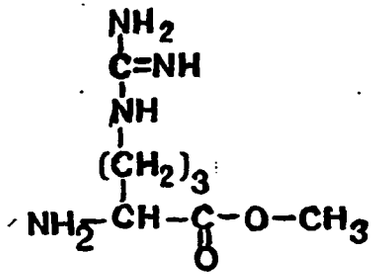

LAME

ENZYME

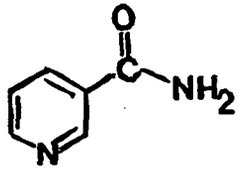

NICOTINAMIDE

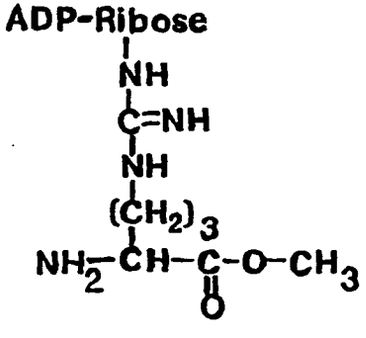

ADP-Ribosylated LAME

(15,16), E. coli LT enterotoxin (17), diphtheria toxin (18), and pertussis toxin (19) elicit their pathogenicity by ADP-ribosylating target proteins in infected cells. Mono-ADP-ribosyl transferase activity has also been reported in lower eukaryotes such as slime molds (20) and upper eukaryotes including avian and human erythrocytes (21,22), rat and chicken liver (23,24) Xenopus tissues (25), canine kidney (26), bovine thyroid (27), and rabbit skeletal muscle (28,29). The widespread occurrence of the transferases has attracted the interest of many research groups who are trying to understand the role that the mono-ADP-ribosyl transferase plays in the regulation of cellular metabolism.

Kharadia and Graves have shown that ADP-ribosylation of Kemptide, a synthetic peptide, suppresses its ability to be phosphorylated by cAMP-dependent protein kinase (30). The relationship between phosphorylation and ADP-ribosylation has also been investigated by Tanigawa and associates. They have shown that ADP-ribosylation suppresses the ability of cAMP-dependent protein kinase to phosphorylate histones and phosphorylase kinase (31). Other metabolic pathways which have been shown to be affected by mono-ADP-ribosylation include: stimulation of thyroid cells by thyrotropin (32), isoproterenol stimulation of hepatocytes (33), and Ca^{2+} release in mitochondria (34).

The existence of hydrolases which specifically cleave ADP-ribose from mono-ADP-ribosylated substrates has also been reported. Hydrolase activity has been described in turkey erythrocytes (35,36), in the photosynthetic nitrogen-fixing bacterium Rhodospirillum rubrum (37), and

in skeletal muscle (38,39); all of which also possess endogenous transferase activity. These reports point strongly toward a highly regulated pathway which utilizes the reversible mono-ADP-ribose modification and its possible interaction with phosphorylation-dephosphorylation pathways.

The specificity of mono-ADP-ribosyltransferases has also been studied. There are three general types of mono-ADP-ribosyl transferases based on the amino acid that is modified on the acceptor substrate. An example of the first type is diphtheria toxin. Diphtheria toxin ADP-ribosylates elongation factor-2 at a diphthamide residue resulting in its inactivation and ultimately cell death (18). Diphthamide is a unique amino acid related to histidine. The second type of mono-ADP-ribosyl transferase specifically modifies cysteine residues. An example of this type is pertussis toxin. Pertussis toxin ADP-ribosylates a cysteine residue on the GTP-binding protein G_i which results in irreversible activation of adenylate cyclase (40). The third type of transferase is represented by cholera toxin which ADP-ribosylates an arginine residue on another GTP-binding protein, G_s (41). Although cholera and pertussis modify two different G proteins, the net effect is the same. The irreversible activation of adenylate cyclase results in an outpouring of ions and water from the cell, also known as diarrhea (15,16).

B. Previous Assays Used

The natural substrates for the endogenous mono-ADP-ribosyl transferases have not been determined. However, the transferases have

been shown to utilize many small molecular weight compounds as artificial substrates. The remainder of this study will be concerned with the assay of arginine specific mono-ADP-ribosyl transferases such as cholera toxin and the transferase found in rabbit skeletal muscle.

ADP-ribosyl transferase activity has been assayed using substrates such as [*a*-^{32}P]NAD (42), [adenine-U-^{14}C]NAD (23,27), or [carbonyl-^{14}C]NAD (16). The incorporation of radioactive ADP-ribose or the release of radioactive nicotinamide was followed by separation of the reaction mixture on a low performance ion-exchange column. However, it has been shown by several groups that the transferases are also capable of hydrolyzing the NAD to free nicotinamide and ADP-ribose in the presence or absence of an acceptor substrate (16,21,23). Therefore, the experiments had to be run in duplicate with and without acceptor so the rate of NAD hydrolysis could be accounted for when the free nicotinamide was measured.

Other studies have utilized specially synthesized model substrates. Mekalanos and co-workers used ^{125}I-guanyltyramine as a low molecular weight acceptor (43). Again, the radioactivity was followed after separation of the product from the unreacted radiolabelled guanyltyramine on a low performance anion exchange column. Soman and associates have synthesized non-radioactive substituted (benzylidineamino) guanidine compounds which absorb light in the UV and visible regions (44,45). The products were separated from the substrates on a reversed-phase HPLC column. Unfortunately, the solubility of these compounds is somewhat low which has limited their usefulness in determining the kinetic parameters

of arginine specific transferases (46).

Arginine containing peptides have been used by Kharadia and Graves for specificity studies. They have shown that small molecular weight substrates which contain a primary amine are also chemically ADP-ribosylated at a site other than the guanidino group (30). Presumably, this occurs through a schiff base type reaction between the primary amine and the free ADP-ribose formed from the hydrolase reaction. The separation and detection scheme must be able to differentiate between the enzymatic and nonenzymatically derived product when using a substrate which contains both a primary amine and the guanidino group.

C. High Performance Liquid Chromatographic Enzyme Assays

A sensitive assay system is required when studying an enzyme. The first enzyme assays utilized the property that the products of enzyme reactions often have different absorbance spectra than the substrates. Dehydrogenases are a good example of this type of system. The UV spectrum of NADH is markedly different than that of the substrate NAD (47,48). However, some enzymes, such as the kinases which utilize ATP and form ADP, cannot be followed by a simple spectroscopic assay because the absorbance spectra of the two adenine containing compounds are so similar. This problem has been overcome by coupling the assay to another enzyme system in which the product of the kinase reaction serves as a substrate for the dehydrogenase reaction (49). When direct or coupled spectroscopic techniques could not be used, the method most often used was radioactive labeling of one of the substrates. However, many of the

radioactive assays employed some type of a time-consuming low performance chromatography step to isolate the product of interest. Examples of these are given earlier in this introduction (16, 23,27 42,43).

Recently, a number of vendors have introduced new bio-compatible HPLC systems which are designed especially for the separation of proteins and peptides and their metabolites (50,51). This fact, along with the advent of more user friendly instrumentation, are the two main reasons that HPLC enzyme assays have become widely used throughout the field of Biochemistry. Literally hundreds of enzymes have been assayed by HPLC methods including those involved in the metabolism of amino acids, carbohydrates, nucleotides, peptides, and proteins (52,53).

One of the advantages of HPLC is that it enables the researcher to follow the changes in concentration of several components of the reaction mixture simultaneously. The components are first separated chromatographically on the column and then detected on-line. Substrate-product pairs which have similar absorbance spectra may then be studied by HPLC without coupling the assay to another system. Development of new stationary phases with improved separation efficiencies has allowed for the detection of enzyme activity in the presence of other enzymes. This eliminates the need for excessive purification before an enzyme may be thoroughly studied. Separation of radioactive components may also be done on a more efficient time scale using HPLC rather than a low performance technique.

Another advantage of using an HPLC assay is that it lends itself readily to a number of different on-line detection schemes. These

include: UV and visible absorption, fluorometry, circular dichroism, refractive index, scintillation counting and various electrochemical methods (54). Thus, HPLC is nearly a universal method for the detection of enzyme activities.

A number of reviews have been written on the use of HPLC in developing enzyme assays (52,55). Sloan has written one which specifically covers the use of HPLC for kinetic analysis (53). It is with these resources and those previously mentioned in this introduction that we embarked on our study of the kinetic mechanism of arginine specific ADP-ribosyl transferases.

II. OBJECTIVES

The objectives of this study were: 1) to develop an assay for arginine specific ADP-ribosyl transferases and 2) to use that assay for the determination of the kinetic mechanism of the transferases. The assay does not require a specially synthesized substrate but rather one that is commercially available in a highly purified form and fairly inexpensive. We did not want to use radiolabelled substrates because of the hazards associated with handling them. An HPLC method was chosen so that we could follow many reaction components simultaneously if we so desired. Another advantage of an HPLC method was rapid sample throughput, as literally hundreds of samples would be analyzed before the study was concluded. For these reasons we chose an assay based on derivatization with a fluorescent tag (ortho-phthaldialdehyde), followed by separation of the mixture on a reversed-phase HPLC column.

Ortho-phthaldialdehyde/2-mercaptoethanol reagent has been primarily used to form fluorescent derivatives with amino acids (56). However, the only requirements for derivatization are the presence of a primary amine and a sulfhydryl agent to form a highly fluorescent isoindole derivative (Figure 2). Derivatization of polar amino acids with OPA/2-mercaptoethanol reagent, prior to injection, allowed them to be separated very efficiently on a reversed-phase column. Unreacted OPA did not interfere with the assay because it did not fluoresce. Figure 3 shows the separation of 22 physiological amino acids in less than 25 minutes. The same mixture would require 60-90 minutes to obtain a

Figure 2. OPA reaction scheme. Reaction goes to completion in 1-2 minutes at room temperature

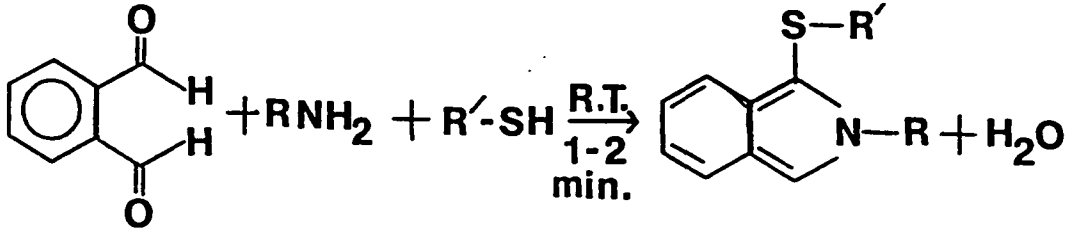

non—fluorescent
o—phthaldialdehyde

highly fluorescent
isoindole

Figure 3. Chromatogram of OPA derivatized amino acids. A mixture of 22 physiological amino acids was mixed with an equal volume of OPA/2-mercaptoethanol reagent for 1 minute at room temperature. The mixture was injected onto a C-8 column at a flow rate of 1.5 ml/min. A gradient elution program of 5% to 65% B in 25 minutes was used to resolve the mixture. The composition of buffers A and B can be found under Methods

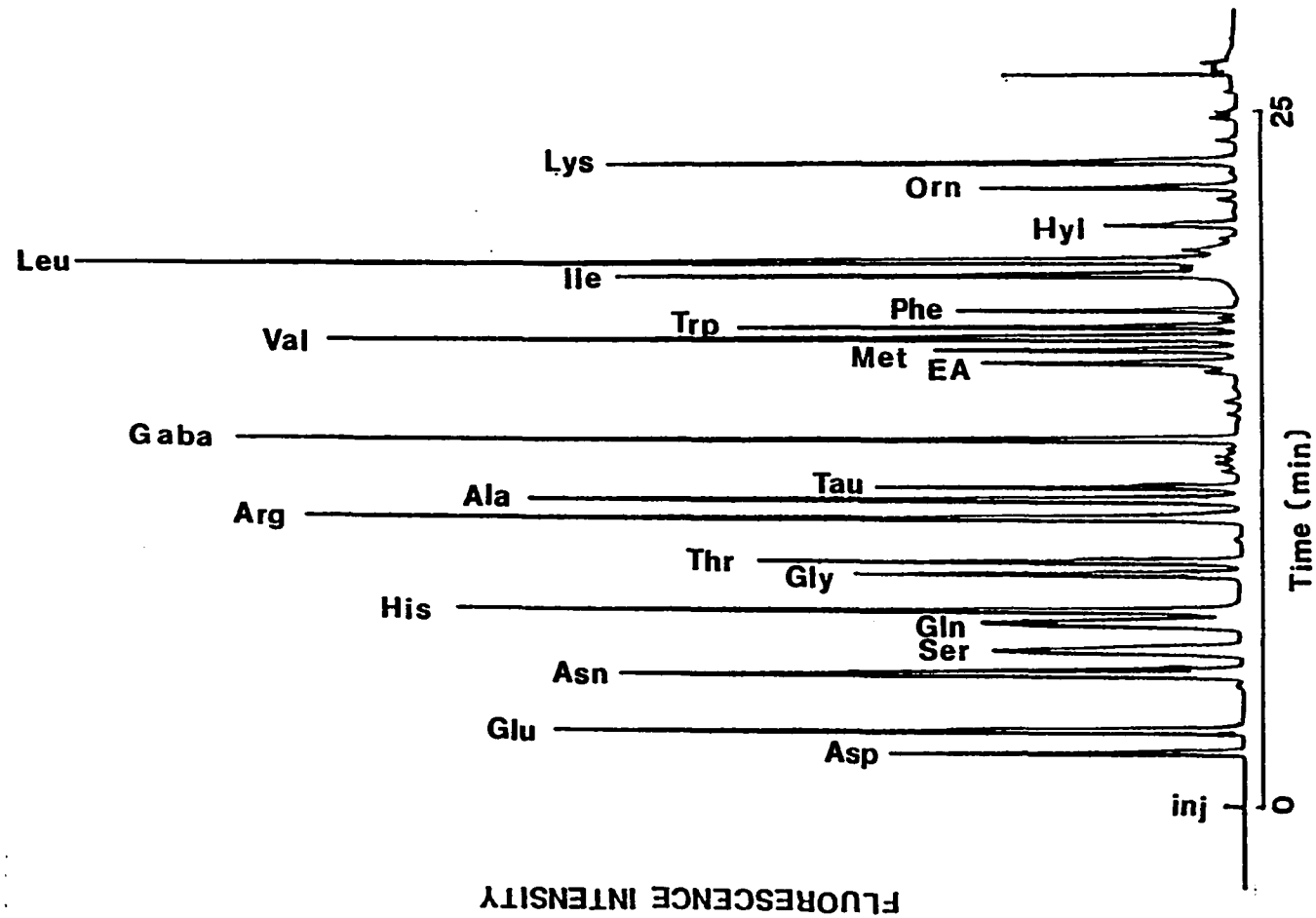
Lys
Orn
Hyl
Leu
Ile
Phe
Trp
Val
Met
EA
Gaba
Tau
Ala
Arg
Thr
Gly
His
Gln
Ser
Asn
Glu
Asp
inj
25
0
Time (min)
FLUORESCENCE INTENSITY

satisfactory separation on an ion exchange column.

It has been shown that the arginine specific ADP-ribose linkage is *a*-N-linked through the guanidino side chain of arginine (57,58). Moss (15,21), Soman (44,45), Mekalanos (43) and their co-workers have shown that small molecular weight guanidino compounds, including arginine and arginine methyl ester, could be utilized as ADP-ribose acceptors in the transferase reaction. We used L-arginine methyl ester as the acceptor substrate in our studies utilizing the free amino group as the site of derivatization with OPA. If the primary amine group on LAME was chemically ADP-ribosylated, it would not be derivatized by the OPA/2-mercaptoethanol reagent and, therefore, would not detected by the fluorescence detector. This property alone obviates the need to run controls for nonspecific chemical ADP-ribosylation reactions such as those observed by Kharadia and Graves (30).

Cholera Toxin A subunit was used as the arginine specific ADP-ribosyl transferase in the development of the assay. This enzyme has been well characterized (43,59,60,61) and was available commercially in a purified, stable and relatively nontoxic form.

III. MATERIALS AND METHODS

A. Materials Used

Cholera Toxin A subunit, NAD, 3-aminobenzamide, L-arginine methyl ester and dithiothreitol were purchased from Sigma (St. Louis, MO). N^G-monomethylarginine was from Calbiochem (San Diego, CA). OPA/2-mercaptoethanol reagent was from Pierce (Rockford, IL). OPA-HR C-8 reversed-phase column was from Alltech (Deerfield, IL). Vydac 301TP anion exchange column was from Anspec (Ann Arbor, MI). HPLC grade tetrahydrofuran, methanol and potassium phosphate buffer salts were from Fisher (Springfield, NJ). All water used for buffer preparations, reagent dilution, and HPLC solvent dilution was deionized to 18 megaohm using a Milli-Q water system from Millipore (Bedford, MA).

B. Methods

1. Purification of rabbit skeletal muscle transferase

The purification of rabbit skeletal muscle transferase was as previously described by Peterson et al.(29). Fractions obtained from the Con A elution step were used in all the muscle transferase assays with at least a ten-fold dilution unless otherwise specified.

2. ADP-ribosyl transferase assay

The ADP-ribosyl transferase assay mixture for cholera toxin contained 50 mM potassium phosphate of pH 7.0, 20 mM DTT, and various amounts of NAD and LAME as indicated. The reaction was initiated with substrate

and incubated at 30°C. Cholera toxin (25 ug/ml) was preactivated for 45 minutes at 30°C in the phosphate-DTT mixture.

The ADP-ribosyl transferase assay mixture for the rabbit skeletal muscle enzyme contained 50 mM potassium phosphate of pH 7.0 and various amounts of NAD and LAME as indicated. The reaction was initiated with enzyme (550 units/ml) and incubated at 30°C. In all assays, the reactions were stopped by pipetting an aliquot of the assay mixture into an equal volume of ice cold 10% TCA and diluted with DI water when necessary. Samples were stable up to two weeks when stored at 4°C.

3. OPA derivatization and HPLC analysis

The HPLC system consisted of two model 110A pumps and a 421 gradient programmer (Beckman; Berkeley, CA). Solvent A was 50 mM potassium phosphate of pH 4.0. Solvent B was 5% THF + 95% methanol. The sample to be analyzed was derivatized with 25 ul of OPA/2-mercaptoethanol reagent for 1 minute and injected onto a 10 cm C-8 reversed-phase column at a flow rate of 1.5 ml/min. The gradient conditions were 5% to 100% B in 5 minutes starting at the time of injection. Total analysis time for each sample was 15 minutes. ADP-ribosylated-LAME had a retention time of 3.9 minutes. Fluorescence was monitored with a Kratos FS 950 fluorometer (ABI; Ramsey, NJ) equipped with a 365 nm bandpass excitation filter and a 418 nm cutoff emission filter.

4. Purification and characterization of product peak

A 24 hour incubation of a cholera toxin mixture was diluted 1:1 with 10% TCA. An aliquot of 200 ul was then injected onto a 25 cm Vydac anion

exchange column. The mixture was eluted isocratically with 50 mM phosphate buffer of pH 2.5. Elution was monitored at 260 nm with a Kratos Spectroflow 757 UV-Vis spectrophotometer (ABI; Ramsey, NJ). The 260 nm absorbing peaks were then analyzed by OPA derivatization for content of the suspected product peak. An absorbance wavelength spectrum was taken of the anion exchange peak which contained the ADP-ribosylated-LAME. The molar absorptivity of ADP-ribose at 260 nm (1500 cm^{-1} M^{-1}) was used to calculate the concentration of the ADP-ribosylated-LAME in the mixture. This concentration was then used to calculate the limit of detection of the assay.

5. Kinetic assays

Initial velocities were determined as a function of varied substrate concentration at several different fixed levels of the second substrate by measuring the amount of product formed over a given time. Time course studies were performed using the highest and lowest substrate concentrations to insure that the velocities were measured in the linear region. Lineweaver-Burk plots were constructed to determine the kinetic parameters. A computer modeling program, developed by Viola (62), that fit the raw data to equations describing various mechanisms was also used to evaluate the kinetic parameters. Inhibitor studies were performed by adding various amounts of 3-aminobenzamide or N^G-monomethylarginine with the substrates when initiating the reactions.

IV. RESULTS AND DISCUSSION

A. Validation of Assay

Cholera toxin A subunit was used as the arginine specific ADP-ribosyl transferase in the development of the assay. The toxin was purchased in a highly purified form to eliminate the possibility of interfering enzymatic activities during the initial stages of assay development. Figure 4 shows a chromatogram obtained from a 1 hour incubation of LAME with cholera toxin. The absence of a peak with a retention time of 3.9 minutes in the zero time (a) and 1 hour control (c) samples indicated that this peak was a product of the cholera toxin reaction. The only products produced in the ADP-ribosylation of LAME by cholera toxin are ADP-ribosylated-LAME and nicotinamide. Since nicotinamide does not contain a primary amine, it could not be derivatized by the OPA/2-mercaptoethanol reagent. Therefore, the only product that could be detected was ADP-ribosylated-LAME.

The appearance of the product was found to be linear with time up to 5 hours as shown in Figure 5. In all stages of the assay development, control reactions were run in which the enzyme or one of the substrates was omitted. This confirmed that the new peak was indeed a product of the enzyme reaction and not simply a breakdown product from one of the components in the reaction mixture.

Purification of the product peak was required before further characterization studies could be attempted. Figure 6a shows the chromatogram obtained from the injection of a 24 hour cholera toxin assay

Figure 4. Chromatograms of OPA derivatized samples from cholera toxin reactions and control mixtures. An aliquot of the cholera toxin assay mixture was mixed with an equal volume of OPA/2-mercaptoethanol for 1 minute at room temperature. The mixture was injected onto a C-8 column at a flow rate of 1.5 ml/min. Elution conditions are described in Methods. Panel a shows the chromatogram from a zero time point sample. Panels b and c are 1 hour time points of cholera toxin reaction mixtures with (b) and without (c) LAME

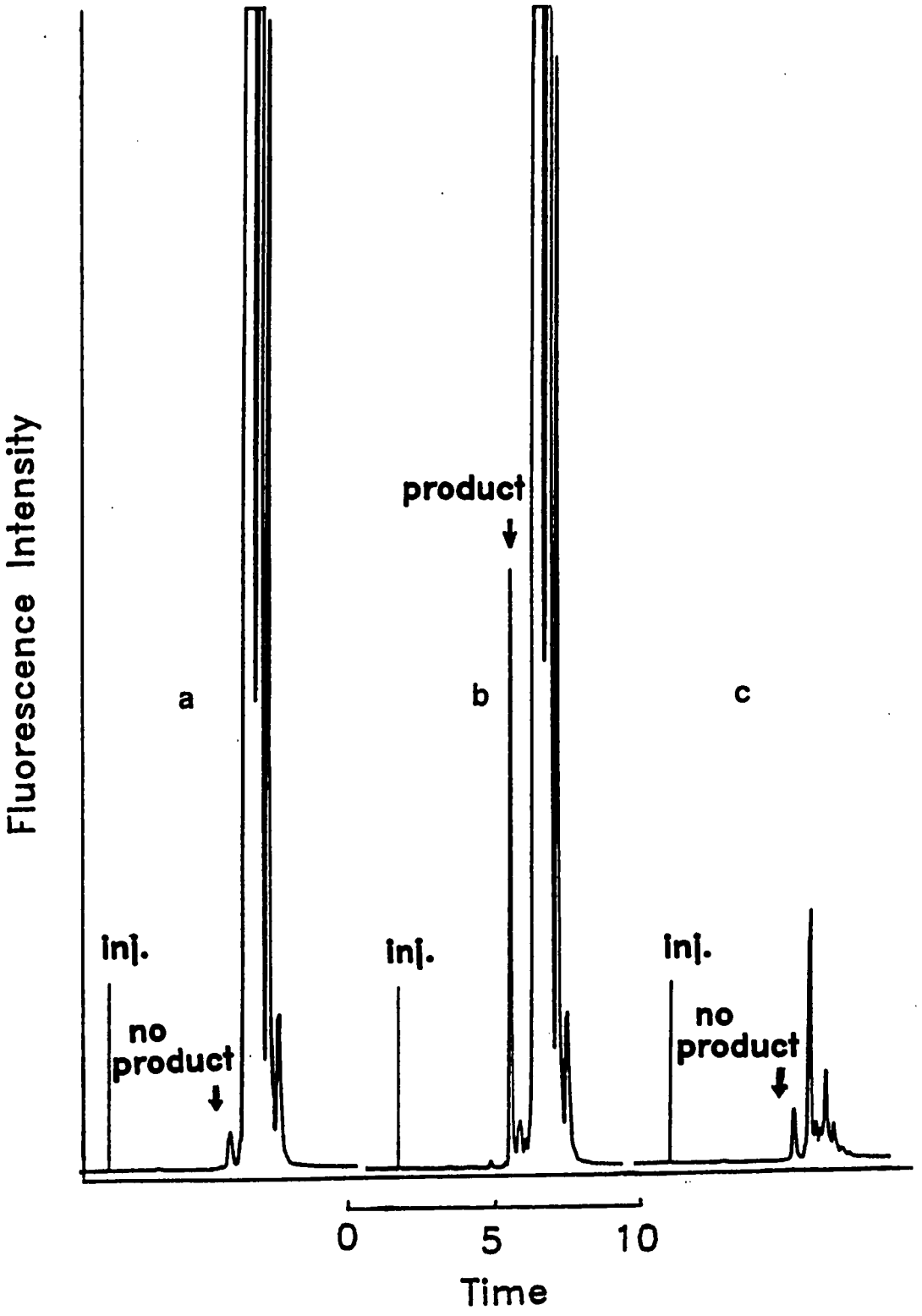
Fluorescence Intensity
product
a
b
c
inj.
no product
inj.
inj.
no product
0
5
10
Time

Figure 5. Time course plot. Cholera toxin (25 ug/ml) was preactivated with DTT as described under Methods. The ADP-ribosylation reaction mixture contained 20 mM DTT, 50 mM LAME, 2 mM NAD, 50 mM potassium phosphate at pH 7.0 and incubated at 30 ^{o}C. Aliquots were removed at various times and the reaction was stopped by the addition of an equal volume of ice cold 10% TCA. Samples were derivatized with an equal volume of OPA/2-mercaptoethanol reagent and injected onto the HPLC system as previously described. The height of the product peak was plotted versus the time at which the reaction was stopped.

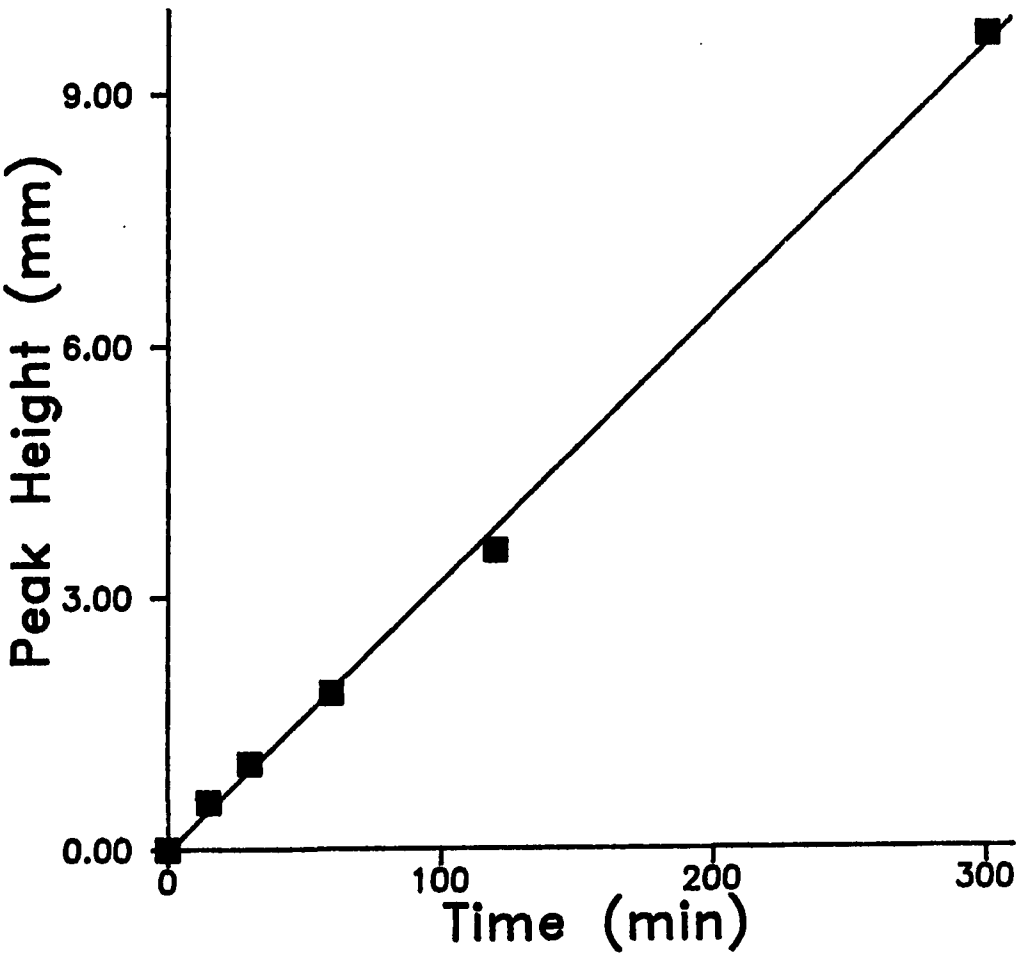
9.00
6.00
3.00
0.00
Peak Height (mm)
0
100
200
300
Time (min)

mixture onto an anion exchange column. Peaks A,B,C, and D absorbed strongly at 260 nm, a wavelength near the maximum absorbance of ADP-ribose. Repeated injections were made and the four separate fractions were collected and pooled. An aliquot of each of the pooled samples was analyzed by OPA/2-mercaptoethanol derivatization to determine which one contained the product of interest. Pool A contained the majority of the product as shown in Figure 6b. Further purification of the product was obtained by reinjecting the pooled A fraction onto the anion exchange column. Spectral analysis of peak A was used to determine the concentration of ADP-ribosylated-LAME by using the extinction coefficient of ADP-ribose at 266 nm. The absorbance spectrum of peak A is shown in Figure 7. Background absorbance was subtracted by scanning a blank which contained the anion exchange eluant. The concentration of ADP-ribosylated-LAME was also determined using acid hydrolysis to release the ADP-ribose moiety, followed by amino acid analysis. The concentration of LAME determined by this method agreed with the calculated concentration of ADP-ribose within $\pm 5\%$. The average of these two values was used as the concentration of ADP-ribosylated-LAME in the standard sample.

An enzyme assay should be able to detect the formation of product in a reaction mixture at very low levels, especially if the assay will be used to monitor the purification of an enzyme. Many enzymes are present at very low levels *in vivo* which makes them quite difficult to detect in the initial purification fractions. Fluorescence methods provide low limits of detection due to low levels of background noise. Figure 8

Figure 6. Anion exchange separation of cholera toxin reaction mixture and OPA derivatization of peak A. A reaction mixture containing 25 ug/ml cholera toxin a subunit, 20 mM DTT 50 mM LAME, 5 mM NAD, and 50 mM potassium phosphate at pH 7.0 was incubated at 30 ^{o}C for 24 hours. An aliquot of the reaction mixture which was diluted 1:1 with 10% TCA was injected onto an anion exchange column. The sample was eluted isocratically with a 50 mM phosphate buffer of pH 2.5. Absorption was monitored at 260 nm (panel a). Peaks A-D were collected separately and analyzed by OPA derivatization with HPLC analysis as described earlier. Panel b shows the chromatogram obtained upon injection of an OPA derivatized sample of peak A.

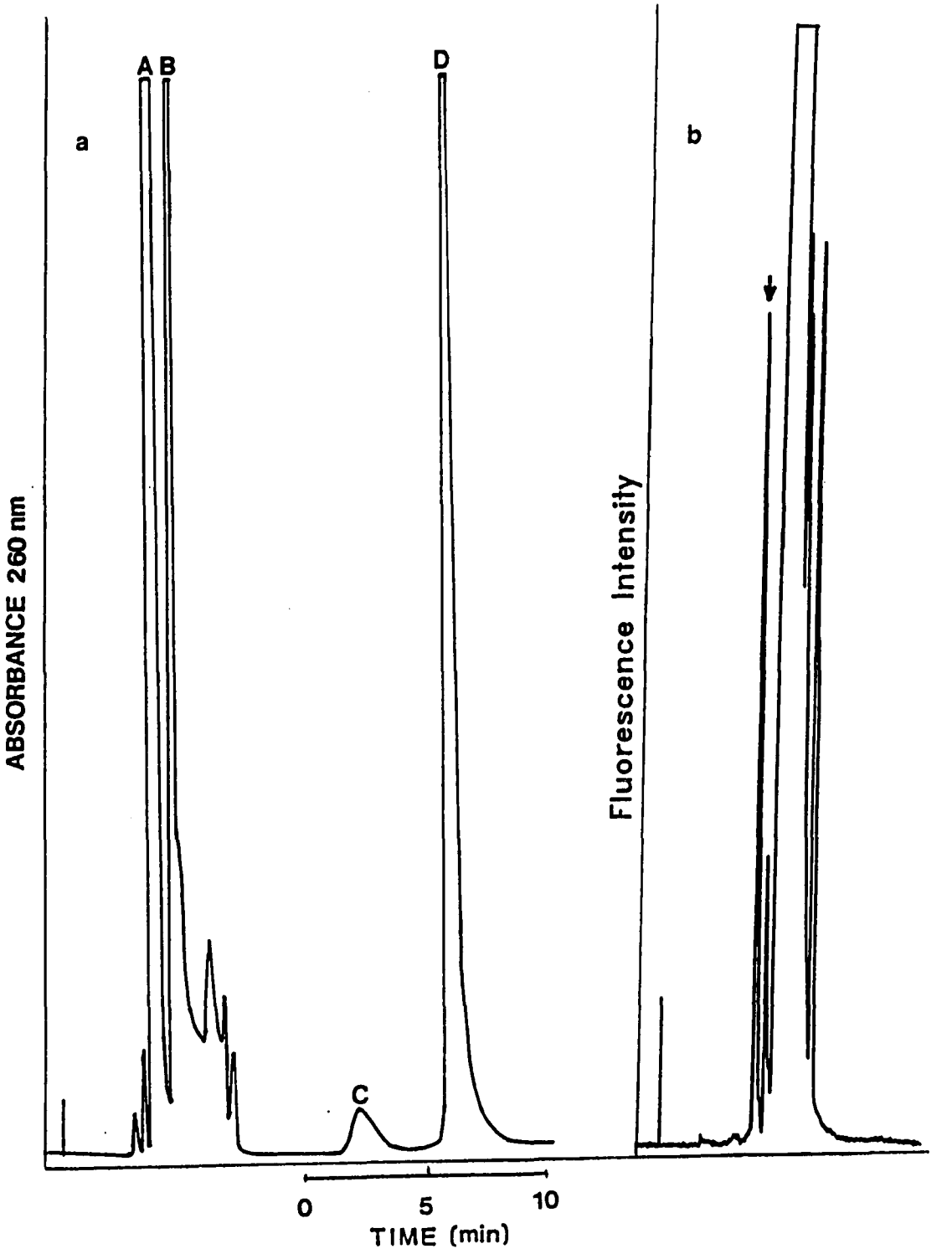
A B
D
a
b
ABSORBANCE 260 nm
Fluorescence Intensity
C
0
5
10
TIME (min)

Figure 7. Absorbance spectrum of peak A. The absorbance spectrum of the reinjected peak A was measured from 200 to 400 nm. A sample of the anion exchange eluant was used to set the blank before obtaining the spectrum of peak A. The absorbance at 266 nm was used to calculate the concentration of ADP-ribosylated-LAME in the sample

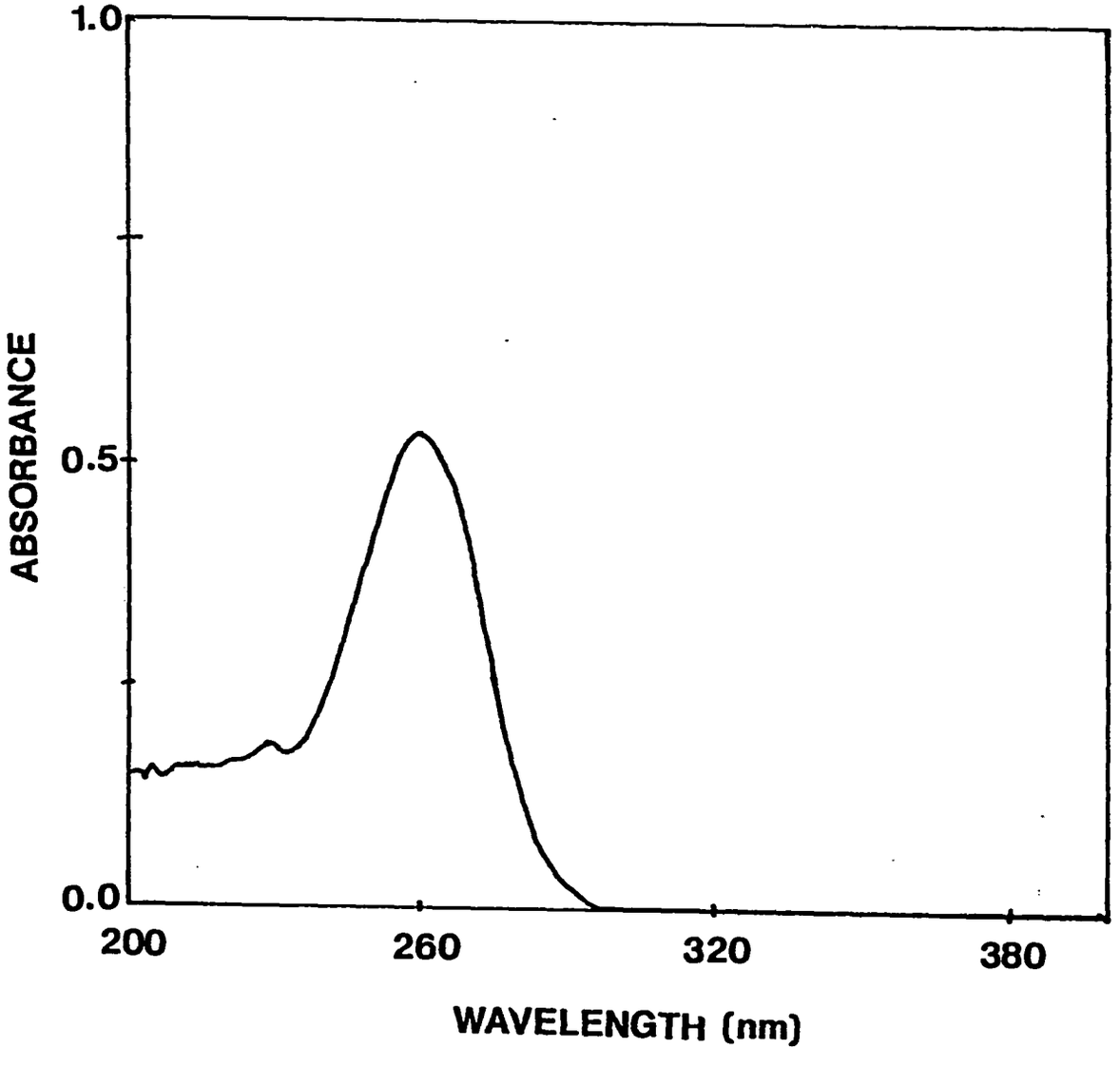
1.0
0.5
0.0
ABSORBANCE
200
260
320
380
WAVELENGTH (nm)

shows the chromatogram obtained upon injection of 600 femtomoles of ADP-ribosylated-LAME, resulting in a limit of detection of 300 femtomoles at a signal to noise ratio of 3. This highly sensitive assay lends itself readily to samples containing very small amounts of arginine specific ADP-ribosyl transferase.

Recently, Peterson and co-workers used the assay in the purification of a transferase from rabbit skeletal muscle (29). This confirmed the ruggedness and adaptability of the assay. Dilution studies proved that the assay was linear with total protein concentration ranging from 0.2 to 2.0 mg/ml, as shown in Figure 9. It could be used from the very first step in the purification, which contained dozens of enzymes, right through to the final affinity chromatography step. Table 1 lists the various steps carried out in the purification of the rabbit muscle enzyme. There was also no apparent interference from detergents used to solubilize the enzyme which is a common problem with UV or visible absorbance techniques.

The DEA-BAG assay, which was developed by Soman and associates (44,45), was previously used to determine the transferase activity. However, it was unable to detect the transferase activity in the final affinity purification step. The turnaround time for the HPLC DEA-BAG assay was approximately 35 minutes. The OPA assay has cut the turnaround time by more than one half, to 15 minutes, allowing for the analysis of more than twice as many samples in the same amount of time. Another advantage of the OPA assay system is the use of a gradient elution program. The DEA-BAG assay uses isocratic elution which creates the

Figure 8. Chromatogram showing the limit of detection. 600 femtomoles of ADP-ribosylated-LAME was derivatized with 25 ul of OPA/2-mercaptoethanol reagent and chromatographed under the conditions described in Methods. The arrow points to the product peak which gives a signal to noise ratio of 6. This resulted in a limit of detection of 300 femtomoles at a signal to noise ratio of 3

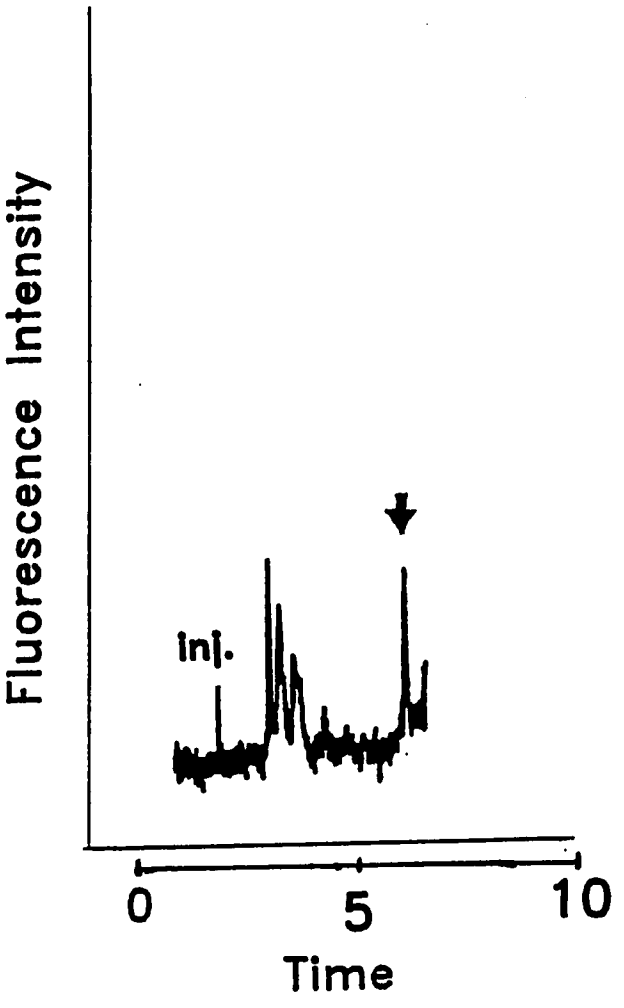
Fluorescence Intensity
inj.
0
5
10
Time

Figure 9. Linear dilution studies. Samples from the 100 k x g supernatant obtained in the purification of rabbit skeletal muscle transferase were diluted to give total protein concentrations ranging from 0.2 to 2.0 mg/ml in the assay mixture. They were incubated with 25 mM LAME, 10 mM NAD, and 50 mM potassium phosphate (pH 7.0) at 30 ^{o}C for 120 minutes. The reactions were stopped with an equal volume of ice cold 10% TCA and derivatized with OPA as previously described. Peak heights of ADP-ribosylated-LAME obtained from the reversed phase HPLC analysis were plotted versus total protein in the reaction mixture

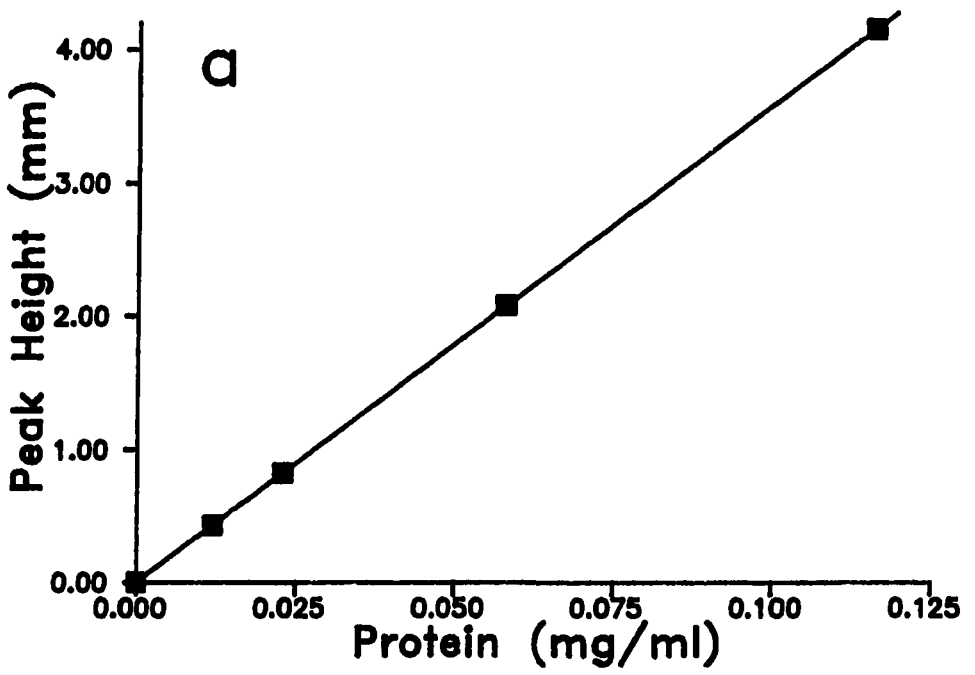
a
Peak Height (mm)
4.00
3.00
2.00
1.00
0.00
0.000
0.025
0.050
0.075
0.100
0.125
Protein (mg/ml)

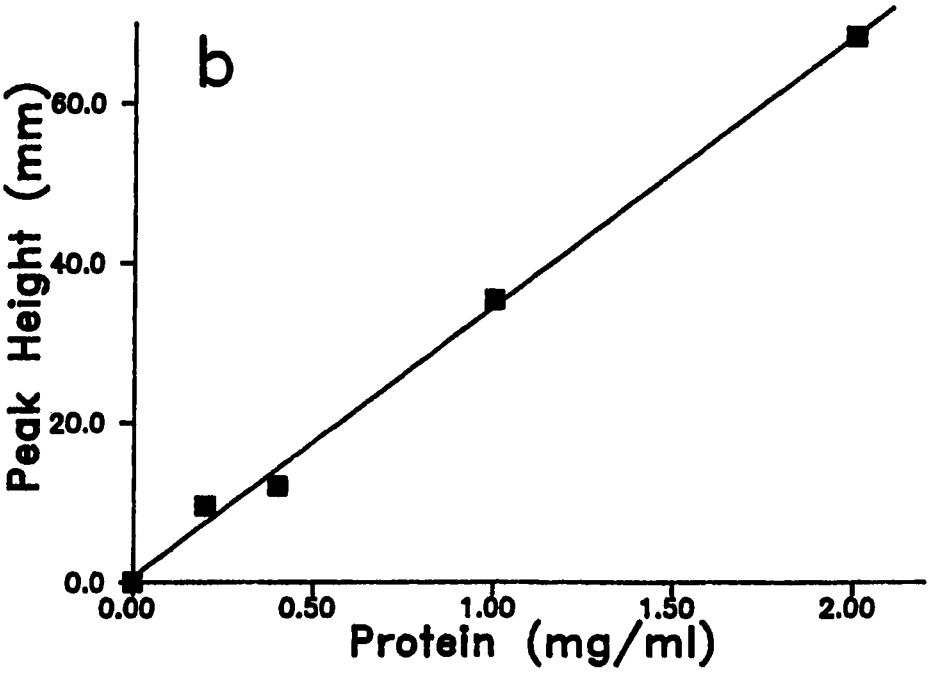
b
Peak Height (mm)
60.0
40.0
20.0
0.0
0.00
0.50
1.00
1.50
2.00
Protein (mg/ml)

Table 1. Summary of the purification of rabbit skeletal muscle transferase[a]

Purification Step	Protein Concentration (mg/ml)	Specific Activity (units/mg)
15 k x g[b] supernatant	12.8	11.5
100 k x g supernatant	11.0	200
Deoxycholate soluble fraction	6.0	294
DE-52 pool	0.26	1160
Con A eluate	0.54	15900
3-ABA eluate	0.01	27400

[a]Adapted from reference 29.

[b]"k x g" = 1000 times the force of gravity.

possibility that late eluting peaks will interfere with subsequent injections. By using a gradient program the column is flushed of all components before the next sample is injected.

B. Determination of Kinetic Parameters

Once the validity of the assay was proved, we were able to proceed with the kinetic portion of the study. The kinetic mechanism of cholera toxin has been studied by a number of investigators. Mekalanos et al. reported an ordered sequential mechanism with K_m values for NAD and ^{125}I-guanyltyramine of 3.6 mM and 44 uM, respectively (43). Their arguments were not very convincing, however, as their double reciprocal plots did not intersect in the same quadrant. Osborne, Stanley, and Moss reported a rapid equilibrium random sequential mechanism for both cholera toxin and the avian erythrocyte enzymes using agmatine as the acceptor substrate (63). However, 1/[agmatine] vs. 1/v plots were not shown for reasons that were not stated in the manuscript.

Our results also supported a sequential mechanism for cholera toxin. The Lineweaver-Burk plots, shown in Figures 10 and 11, resulted in a pattern of nonparallel lines which intersected at one common point in the lower left quadrant. This type of intersection pattern is indicative of a sequential rather than a ping pong type mechanism. The two different mechanisms are illustrated in Figures 12 and 13 (64). Figure 12 represents the sequential mechanism where both substrates must bind to the enzyme before any product is produced. However, as shown in Figure 13, a ping pong mechanism is one where the first substrate binds and a

Figure 10. Double reciprocal plot of initial velocity versus LAME concentration at constant NAD concentrations using cholera toxin. The reciprocal of the initial velocities at various constant levels of NAD were plotted as a function of the reciprocal of LAME concentration. The incubation mixtures contained 25 ug/ml of activated cholera toxin, 50 mM potassium phosphate pH 7.0, 20 mM DTT, and LAME. NAD concentrations were: ■ 0.75 mM, ▲ 1.5 mM, ● 3.0 mM, ★ 6.0 mM

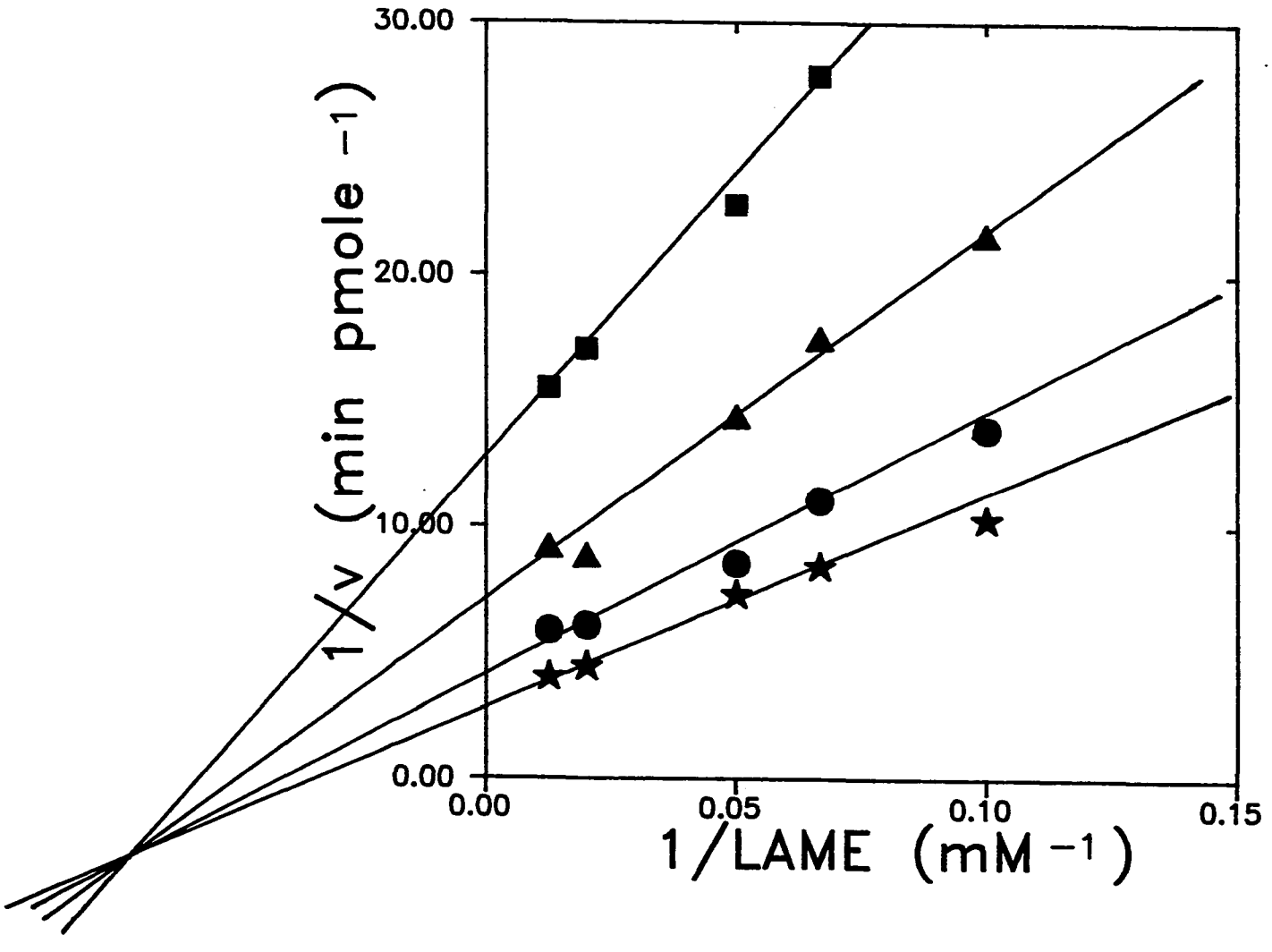
30.00
20.00
10.00
0.00
1/v (min pmole -1)
0.00
0.05
0.10
0.15
1/LAME (mM -1)

Figure 11. Double reciprocal plot of initial velocity versus NAD concentration at constant LAME concentrations using cholera toxin. The reciprocal of the initial velocities at various constant levels of LAME were plotted as a function of the reciprocal of NAD concentration. The incubation mixtures contained 25 ug/ml of activated cholera toxin, 50 mM potassium phosphate pH 7.0, 20 mM DTT, and NAD. The LAME concentrations were: ● 10 mM, ■ 15 mM, ▲ 20mM, ★ 50 mM

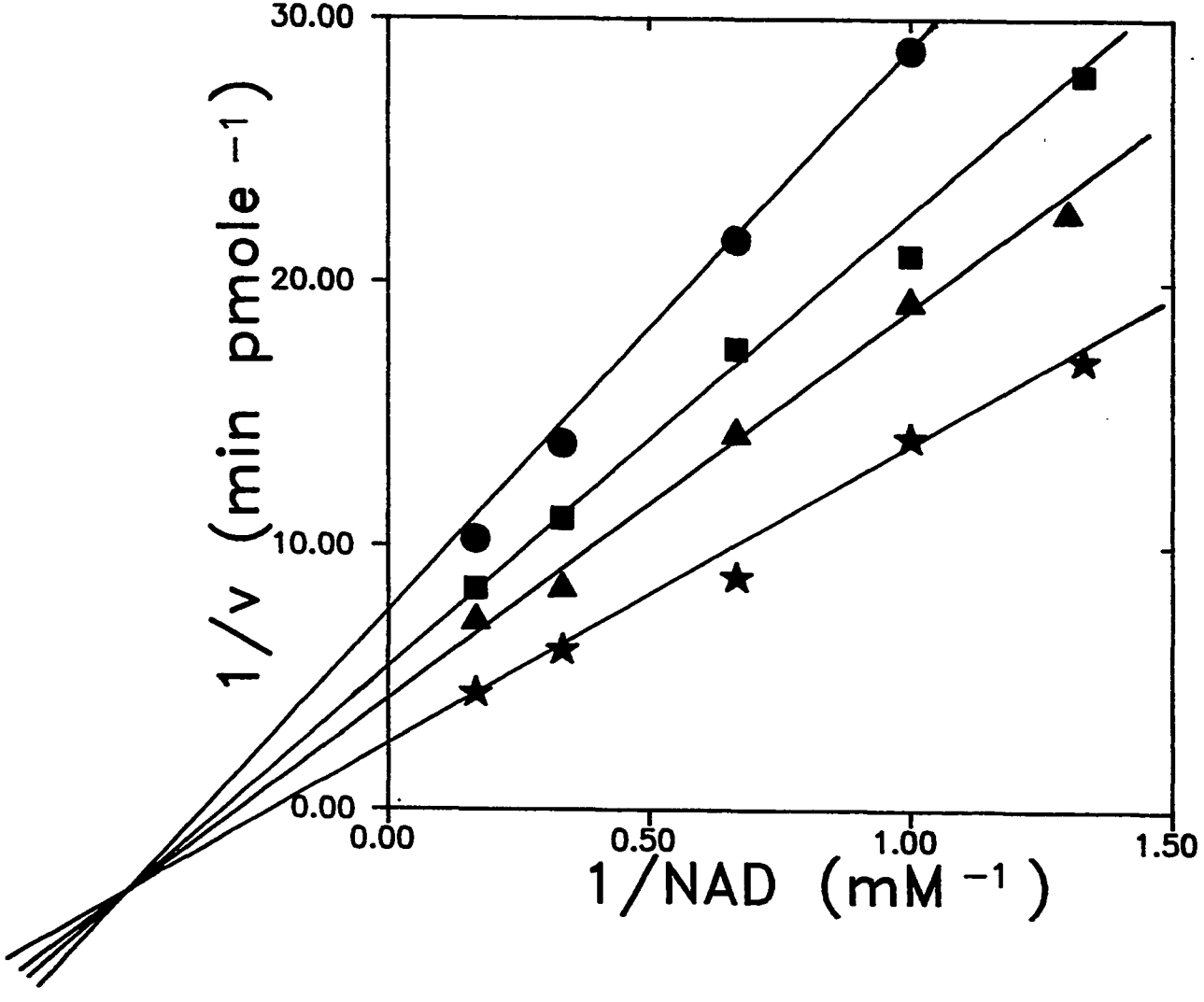
30.00
20.00
10.00
0.00
1/v (min pmole -1)
0.00
0.50
1.00
1.50
1/NAD (mM -1)

Figure 12. Sequential mechanism scheme. This is a scheme representing a sequential mechanism involving an enzyme (E), two substrates (A and B), and two products (P and Q). Adapted from reference 64

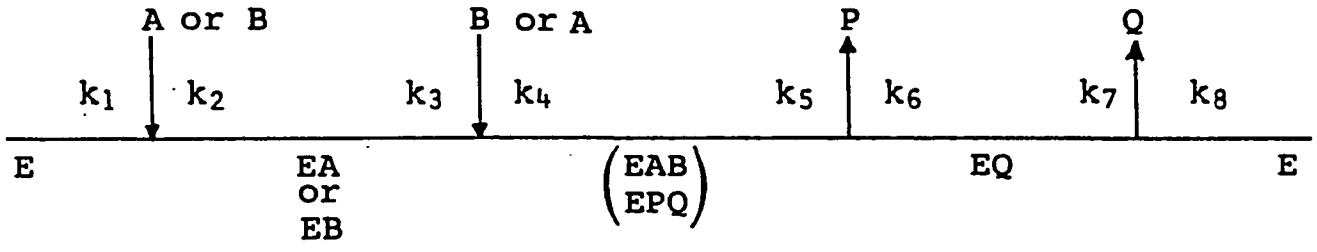
A or B
B or A
P
Q
k1
k2
k3
k4
k5
k6
k7
k8
E
EA
or
EB
EAB
EPQ
EQ
E

Figure 13. Ping Pong mechanism scheme. This scheme represents a ping pong mechanism involving an enzyme (E), two substrates (A and B), and two products (P and Q). Adapted from reference 64

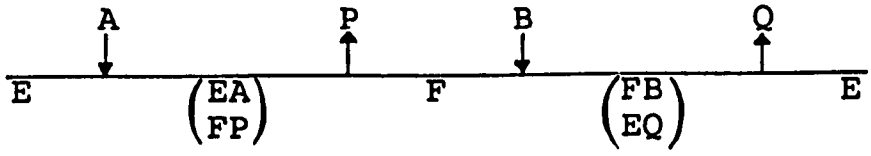
A
P
B
Q
E
EA
FP
F
FB
EQ
E

product is formed, before the second substrate binds.

The same type of experiments were performed using a preparation of the rabbit skeletal muscle transferase. In these assays the fraction obtained from the Con A affinity step was used. This fraction was shown to contain over 50% transferase with relatively few remaining proteins (29). The final 3-ABA affinity fraction was not used because of the extremely low yield of enzyme. As shown in Figures 14 and 15, double reciprocal plots for this enzyme also showed a pattern indicative of a sequential mechanism. The linear nature of the Lineweaver-Burk plots, obtained with cholera toxin and the rabbit skeletal muscle enzyme, indicates that they both obey Michaelis-Menten type kinetics.

The secondary plots constructed from the slopes and intercepts of the Lineweaver-Burk plots are shown in Figures 16-19. Figures 16 and 17 show the secondary plots obtained when using cholera toxin. The secondary plots obtained when using the rabbit skeletal muscle transferase are shown in Figures 18 and 19. The intersection point of the lines with the abscissa on the intercept plots give the Michaelis constant of the substrate at infinite concentration of the other substrate. The maximal velocity in the forward direction, at infinite concentration of both substrates, is calculated from the intersection point on the ordinate of the intercept plot. The same parameters may also be obtained from the slope plots. The kinetic parameters calculated from these plots were compared and averaged with those obtained from the computer modeling program (62). The formulae of the rate equations used for the calculation of these results are found in the Appendix.

Figure 14. Double reciprocal plot of initial velocity versus LAME concentration at constant NAD concentrations using rabbit skeletal muscle transferase. The reciprocal of the initial velocities at various constant levels of NAD were plotted as a function of reciprocal of LAME concentration. The incubation mixtures contained 5 ug/ml rabbit muscle transferase (Con A fraction), 50 mM potassium phosphate pH 7.0, and LAME. The concentrations of NAD were: ★ 25 uM, ■ 50 uM, ▲ 75 uM, ● 100 uM

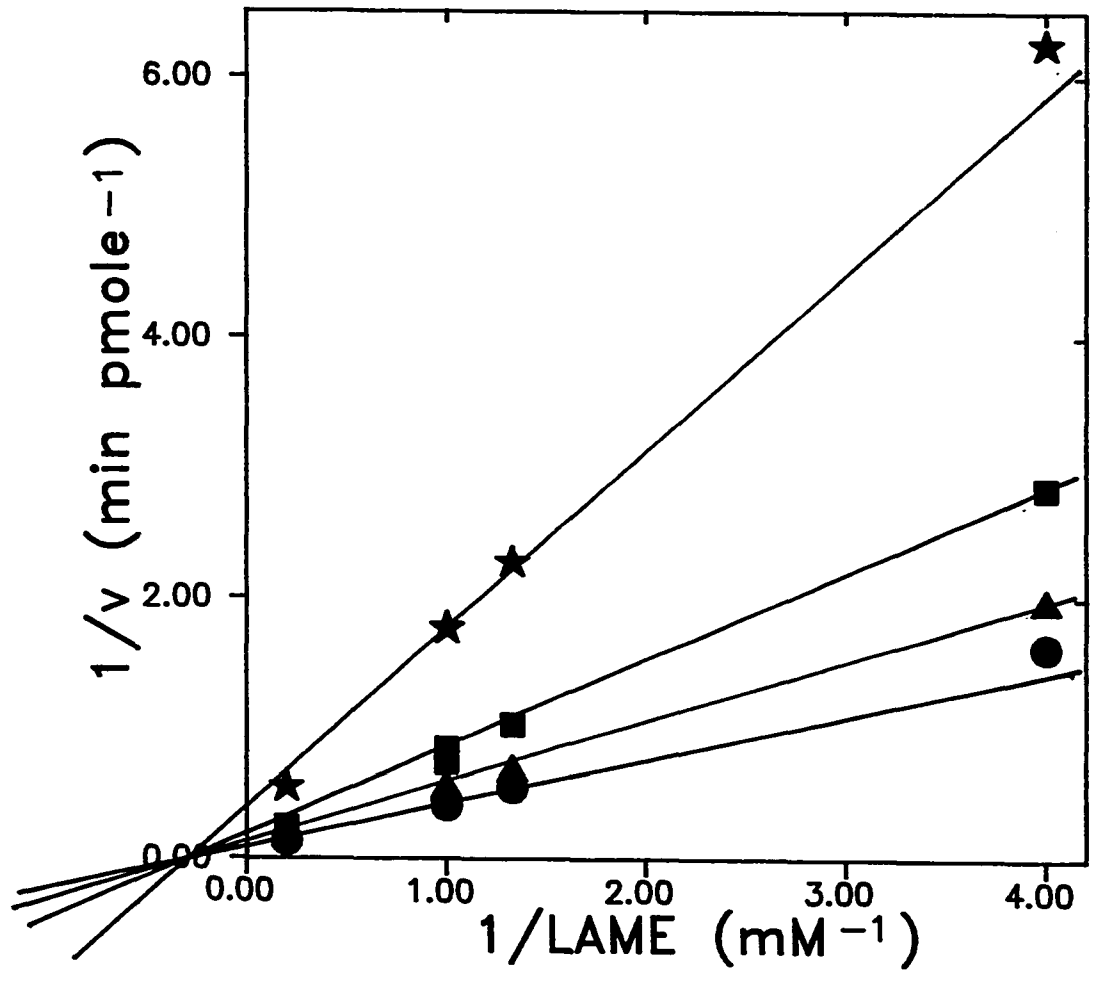
6.00
4.00
2.00
0.00
1/v (min pmole-1)
0.00
1.00
2.00
3.00
4.00
1/LAME (mM-1)

Figure 15. Double reciprocal plot of initial velocity versus NAD concentration at constant LAME concentrations using rabbit skeletal muscle transferase. The reciprocal of the initial velocities at various constant levels of LAME were plotted as a function of NAD concentration. The incubation mixture contained 5 ug/ml of rabbit muscle transferase (Con A fraction), 50 mM potassium phosphate, and NAD. The LAME concentrations were: ■ 0.25 mM, ● 0.75 mM, ★ 1.0 mM, ▲ 5.0 mM

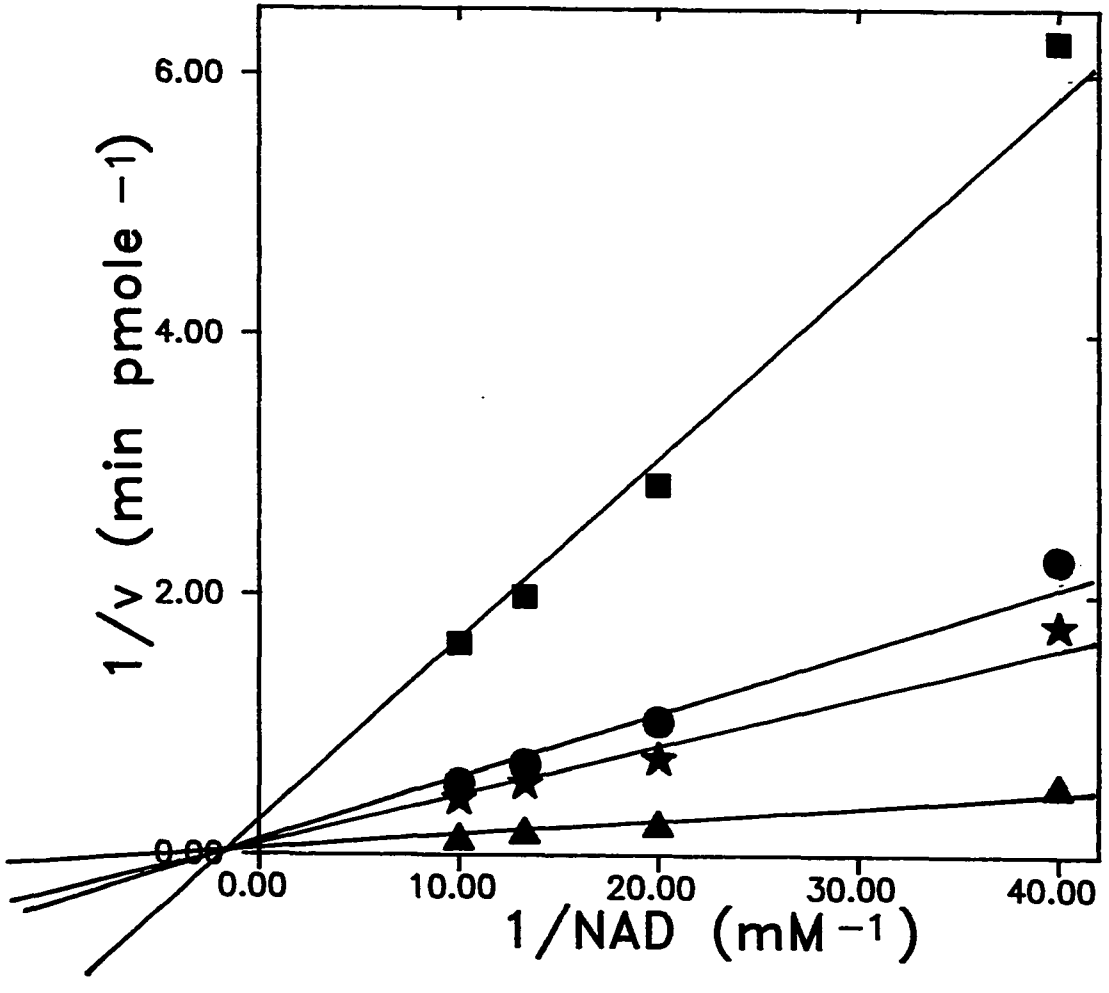
6.00
4.00
2.00
0.00
1/v (min pmole −1)
0.00
10.00
20.00
30.00
40.00
1/NAD (mM −1)

Figure 16. Secondary slope plots for cholera toxin. Slopes of the family of lines in Figures 10 were plotted versus the reciprocal of NAD concentration (a) and slopes of the family of lines in Figure 11 were plotted versus the reciprocal of LAME concentration (b)

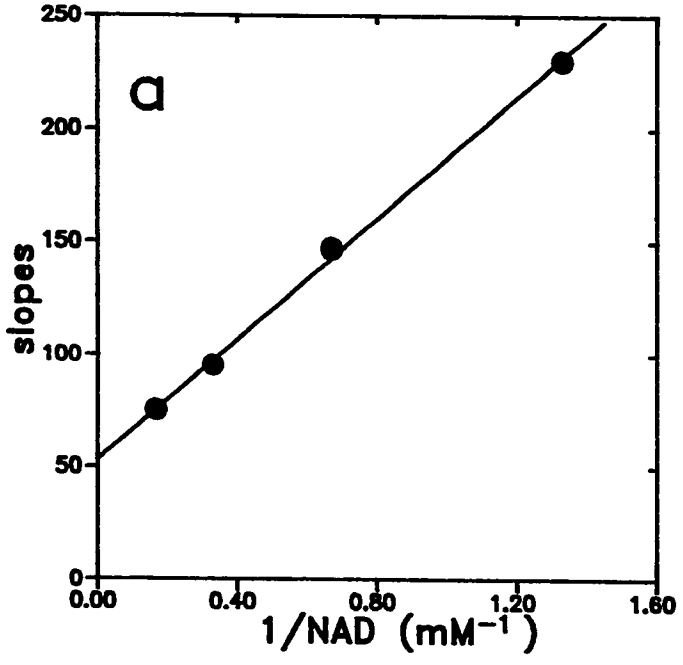
a
slopes
250
200
150
100
50
0
0.00
0.40
0.80
1.20
1.60
1/NAD (mM^{-1})

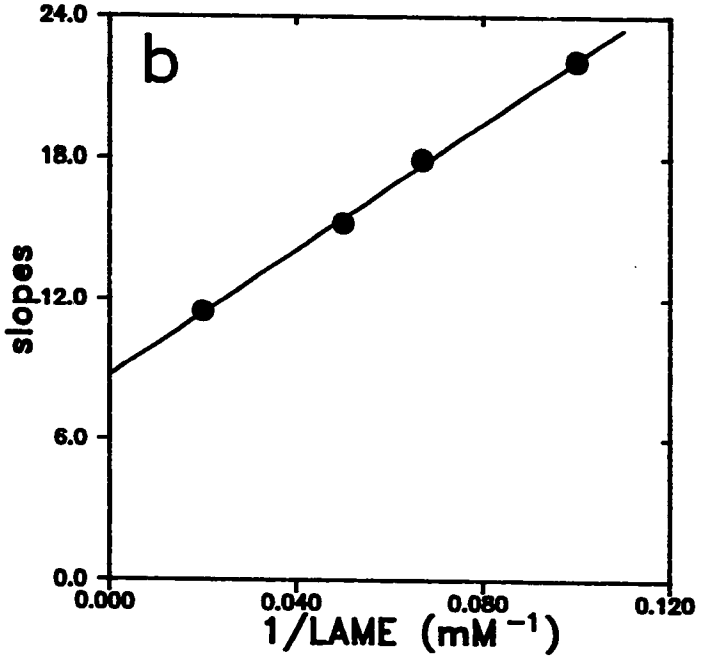
b
slopes
24.0
18.0
12.0
6.0
0.0
0.000
0.040
0.080
0.120
1/LAME (mM^{-1})

Figure 17. Secondary intercept plots for cholera toxin. Intercepts with the 1/v axis of Figure 10 were plotted versus the reciprocal of NAD concentration (a) and intercepts with the 1/v axis of Figure 11 were plotted versus the reciprocal of LAME concentration

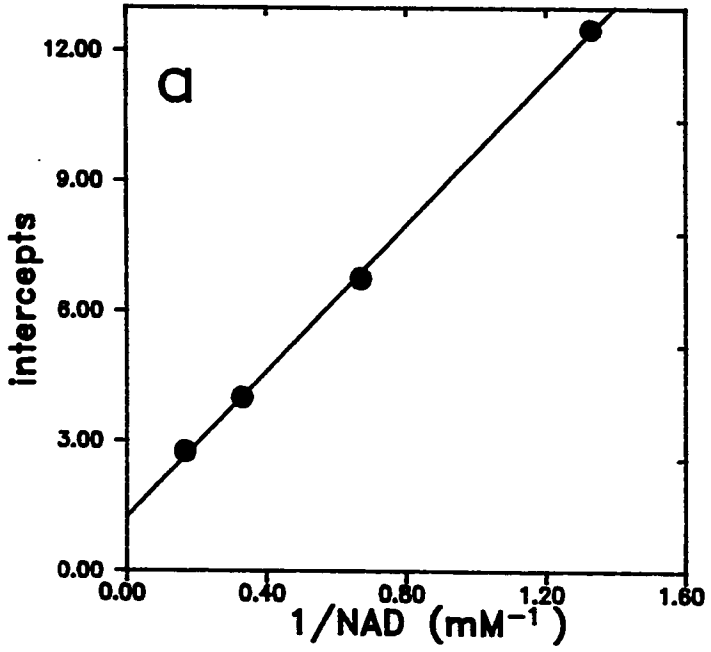
a
12.00
9.00
6.00
3.00
0.00
intercepts
0.00
0.40
0.80
1.20
1.60
1/NAD (mM^{-1})

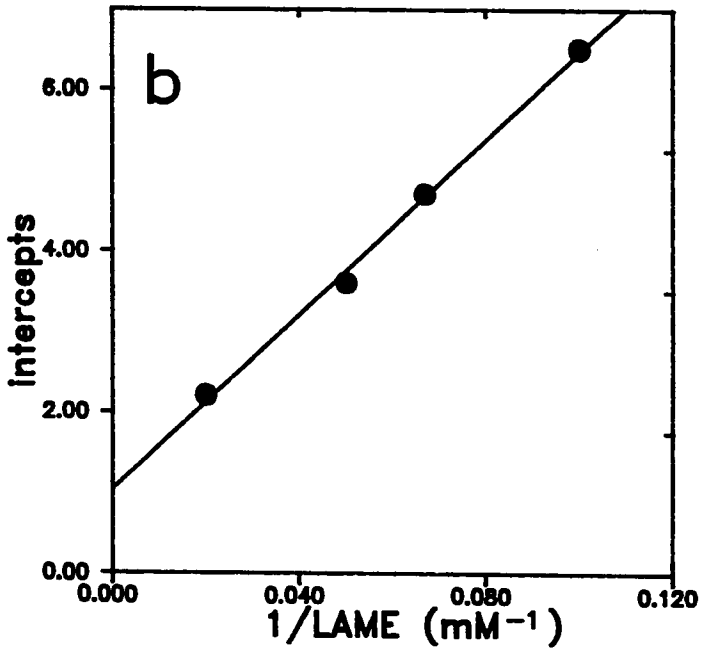
b
6.00
4.00
2.00
0.00
intercepts
0.000
0.040
0.080
0.120
1/LAME (mM^{-1})

Figure 18. Secondary slope plots for rabbit skeletal muscle transferase. Slopes of the family of lines in Figure 14 were plotted as a function of the reciprocal of NAD concentration (a) and slopes of the family of lines in Figure 15 were plotted as a function of the reciprocal of LAME concentration (b)

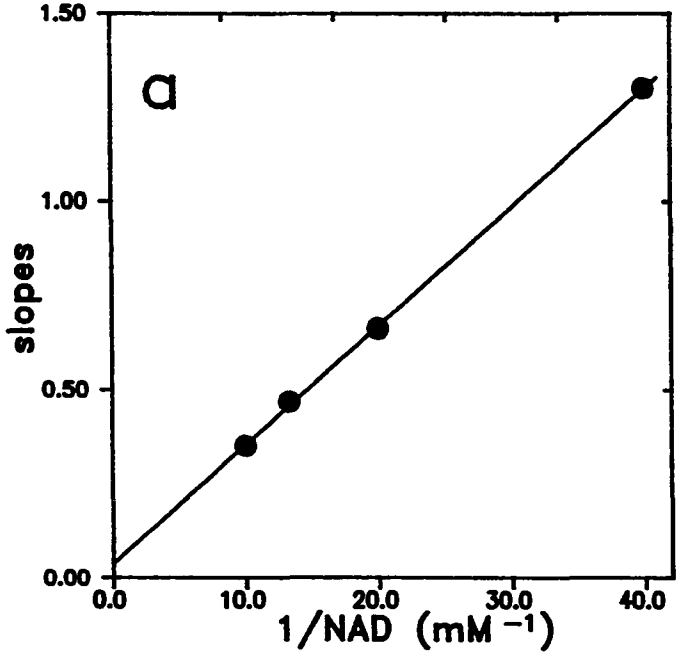
a
slopes
1.50
1.00
0.50
0.00
0.0
10.0
20.0
30.0
40.0
1/NAD (mM $^{-1}$)

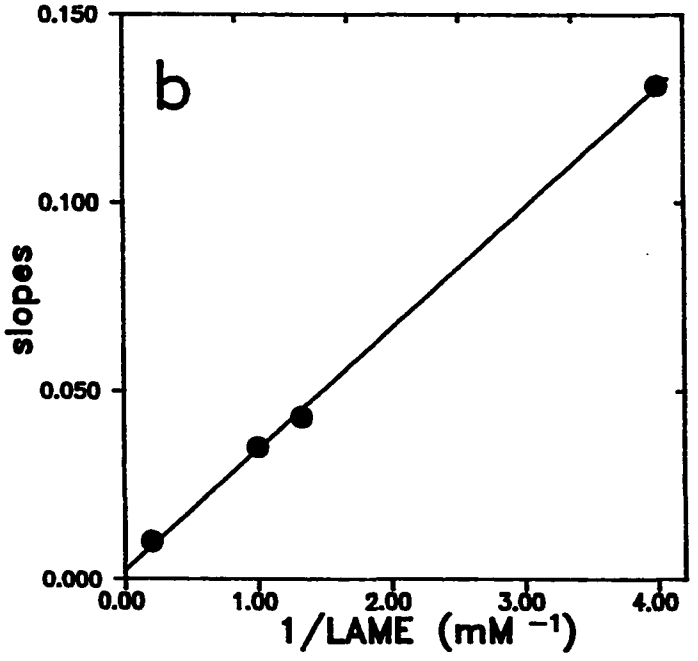
b
slopes
0.150
0.100
0.050
0.000
0.00
1.00
2.00
3.00
4.00
1/LAME (mM $^{-1}$)

Figure 19. Secondary intercept plots for rabbit skeletal muscle transferase. Intercepts with the 1/v axis of Figure 14 were plotted as a function of the reciprocal NAD concentration (a) intercepts with the 1/v axis of Figure 15 were plotted as a function of the reciprocal LAME concentration (b)

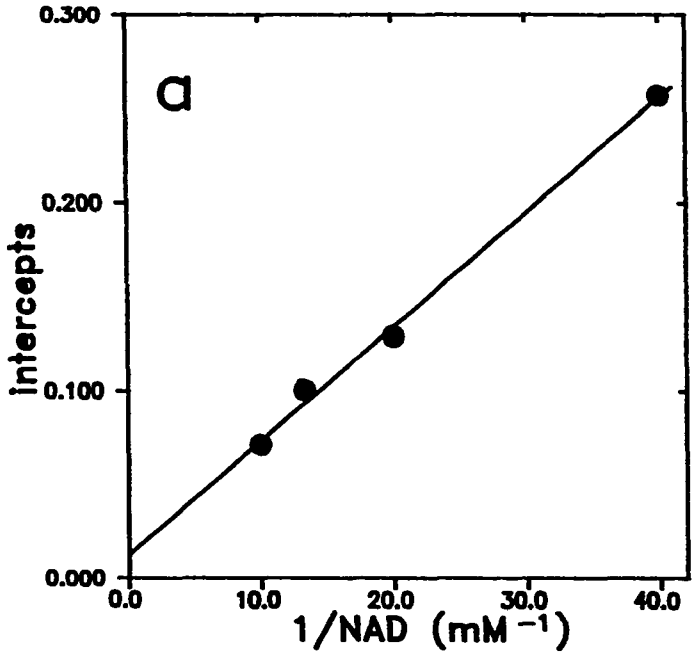
a
0.300
0.200
0.100
0.000
Intercepts
0.0
10.0
20.0
30.0
40.0
1/NAD (mM^{-1})

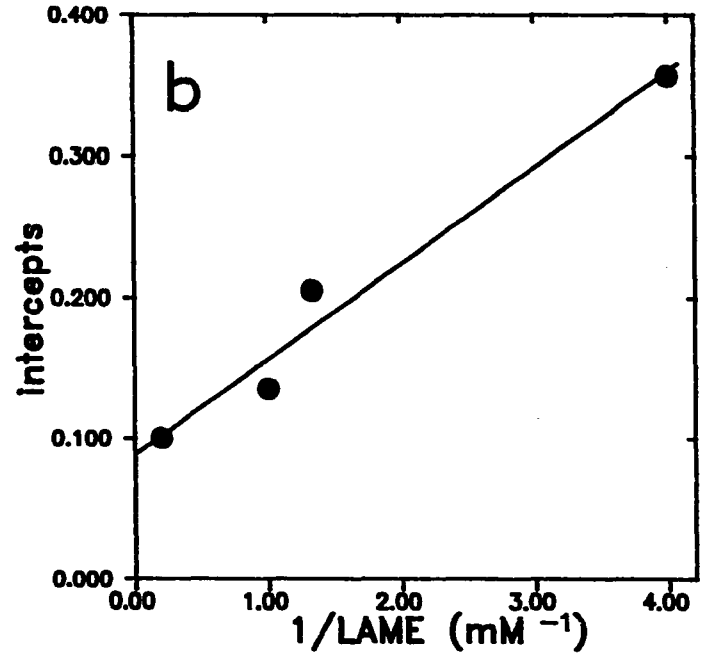
b
0.400
0.300
0.200
0.100
0.000
Intercepts
0.00
1.00
2.00
3.00
4.00
1/LAME (mM^{-1})

The values of kinetic parameters for cholera toxin, determined by various investigators, are listed in Table 2. Our K_m results for cholera toxin, of 5.6 mM for NAD and 39 mM for LAME, agree very well with those previously reported. The reported V_{max} value of 0.5 umoles min^{-1} mg^{-1} also corresponds rather closely to that obtained by other groups. The endogenous rabbit muscle transferase resulted in K_m values which were somewhat higher than those reported by Osborne for the avian erythrocyte enzyme as shown in Table 3. This difference is most likely due to the fact that the avian transferase was obtained from the soluble cell fraction, whereas, the rabbit transferase was isolated from the membrane fraction. The soluble and membrane enzymes would presumably play two very different roles in regulating cellular metabolism. Therefore, they would be expected to have significantly different affinities toward the same substrate as reflected in the values reported in Table 3.

Thus, from initial rate studies using both cholera toxin and rabbit skeletal muscle transferase, it can be concluded that both enzymes catalyze ADP-ribosylation in a manner consistent with a sequential mechanism (i.e., products are released from the enzyme only after both substrates are bound). The sequential model is described by the following rate equation:

$$\frac{1}{v} = \frac{1}{V_1} + \frac{K_a}{V_1(A)} + \frac{K_b}{V_1(B)} + \frac{K_{ia} K_b}{V_1(A)(B)} \qquad (1)$$

Table 2. Kinetic parameters of cholera toxin

K_m, NAD (mM)	K_m, ADP-ribose acceptor (mM)	V_{max} ($\frac{umole}{min\ mg}$)	Reference
1.1	35[a]	28	(63)
3.6	0.044[b]	NR[c]	(43)
NR	75[d]	NR	(43)
5.6	39[e]	0.50	this study
1.9	17[f]	0.051	this study

[a]Using agmatine.

[b]Using guanyltyramine.

[c]Not reported.

[d]Using arginine.

[e]Using LAME.

[f]Using canavanine.

Table 3. Kinetic parameters of endogenous transferases

	Avian Erythrocyte Transferase[a]	Rabbit Skeletal Muscle Transferase[b]
K_m, NAD	7.0 uM	0.56 mM
K_m, acceptor	0.26 mM	1.2 mM
V_{max}	31 $\frac{\text{umole}}{\text{min mg}}$	40 $\frac{\text{umole}}{\text{min mg}}$

[a]From reference (63) using agmatine.

[b]From this study using LAME.

C. Inhibitor Studies

Once it was established that the two enzymes did indeed follow a sequential type of mechanism, inhibitor studies were conducted to determine if the mechanisms were random or ordered. The random sequential mechanism is depicted in Figure 20 (64). Here, there is no obligatory order in which the substrates bind to the enzyme. Compare this to the ordered mechanism, shown in Figure 21, where one substrate, A, must bind to the enzyme before the second substrate can be bound and a productive ternary complex formed (64). It was this characteristic of the cholera toxin mechanism which seemed to be most refuted in the literature.

As stated earlier Mekalanos reported an ordered mechanism (43) but Osborne had reported a random type (63). Neither one of these two studies were very convincing. Mekalanos had problems in the initial stages of his study because he was not able to obtain Lineweaver-Burk plots that intersected in the same quadrant. Osborne and co-workers obtained satisfactory results in the initial stages but did not conduct complete inhibition studies. Product inhibition was studied using only one product, nicotinamide. An estimate was made as to what extent the apparent inhibition constant for nicotinamide depended upon the concentration of the acceptor substrate. The choice of random vs. ordered was based on whether this factor was or was not equal to 1.

A more direct method of differentiating between ordered and random sequential mechanisms is described by Fromm (64). In this type of study

Figure 20. Random sequential mechanism scheme. This scheme represents a random sequential mechanism for an enzyme (E), two substrates (A and B), and two products (P and Q). Adapted from reference 64

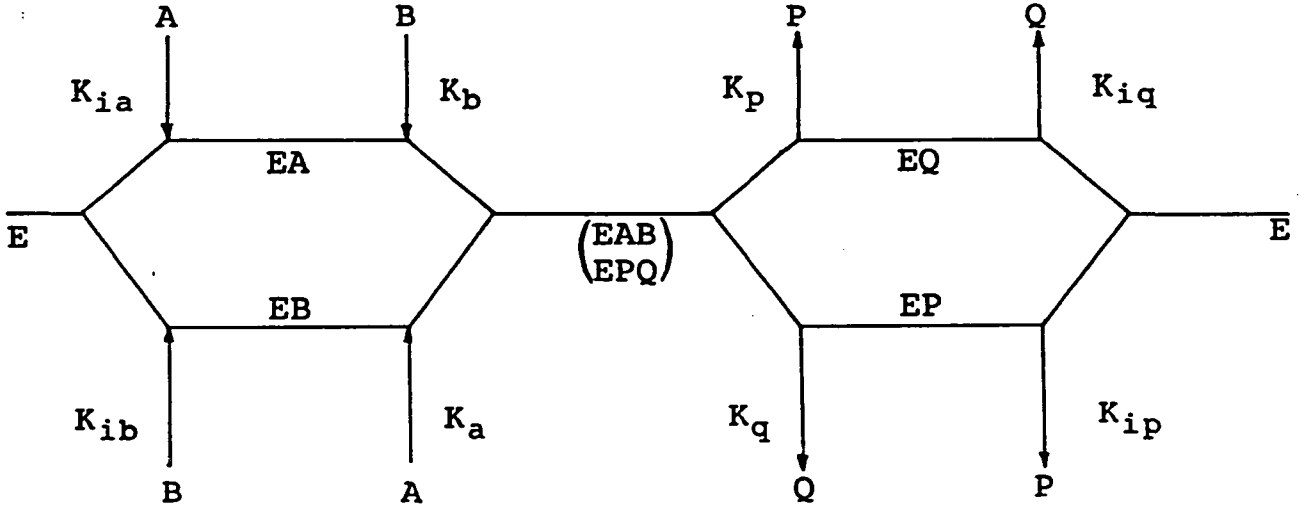
A
B
P
Q
K_{ia}
K_b
K_p
K_{iq}
EA
EQ
E
(EAB / EPQ)
E
EB
EP
K_{ib}
K_a
K_q
K_{ip}
B
A
Q
P

Figure 21. Ordered sequential mechanism. This scheme represents an ordered sequential mechanism for an enzyme (E), two substrates (A and B), and two products (P and Q). Adapted from reference 64

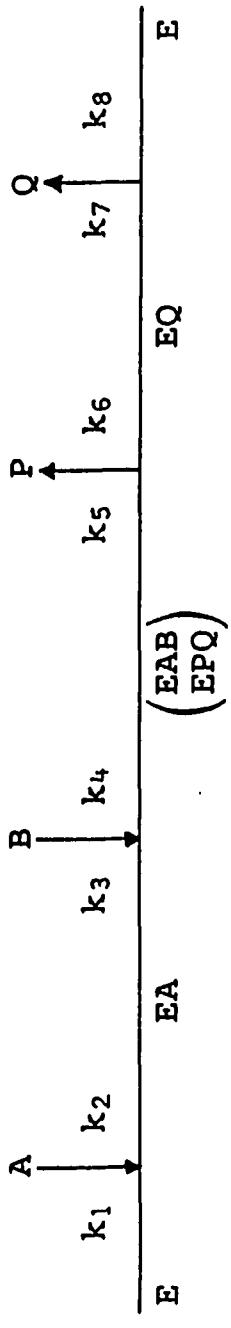
E
k8
Q
k7
EQ
k6
P
k5
(EAB EPQ)
k4
B
k3
EA
k2
A
k1
E

an investigator is able to determine the type of mechanism based on how the initial velocities are affected when specific inhibitors are added to the reaction mixture. One of the inhibitors must be competitive toward the ADP-ribose donor substrate and the other must be competitive against the acceptor substrate. Narayanan attempted these types of inhibition studies using substituted (benzylidineamino) guanidine compounds as the acceptor substrate (46). However, the solubility of these compounds and their apparent inhibition at higher concentrations did not allow complete kinetic analyses to be conducted.

We performed the inhibition studies using the HPLC OPA assay described earlier. The compound chosen to test against competitiveness toward NAD was 3-aminobenzamide. This compound had been used in previous studies by other investigators and was shown to be a good inhibitor in both mono- and poly-ADP-ribosyl transferase reactions (65,66). Figure 22 shows the results obtained for cholera toxin when increasing amounts of 3-aminobenzamide were incubated with various amounts of NAD and a constant amount of LAME. The results of these same experiments using rabbit skeletal muscle transferase are shown in Figure 23. The convergence of the lines to a single point on the 1/v axis is indicative of competitive inhibition toward NAD. Both enzymes exhibited the same type of behavior, resulting in a K_I of 35 mM for cholera toxin and 14 mM for the rabbit skeletal muscle enzyme.

A pattern of noncompetitive inhibition was observed when a constant amount of NAD was incubated with varying amounts of LAME and increasing amounts of 3-aminobenzamide. Noncompetitive inhibition is

Figure 22. Double reciprocal plot of initial velocity versus NAD concentration at constant 3-aminobenzamide concentrations using cholera toxin. The reciprocal of the initial velocities at various constant levels of 3-aminobenzamide were plotted as a function of the reciprocal of NAD concentration. The incubation mixture contained 25 ug/ml of activated cholera toxin, 50 mM potassium phosphate pH 7.0, 20 mM DTT, 20 mM LAME, and NAD. The 3-aminobenzamide concentrations were: ● 0 mM, ▲ 10 mM, ■ 20 mM

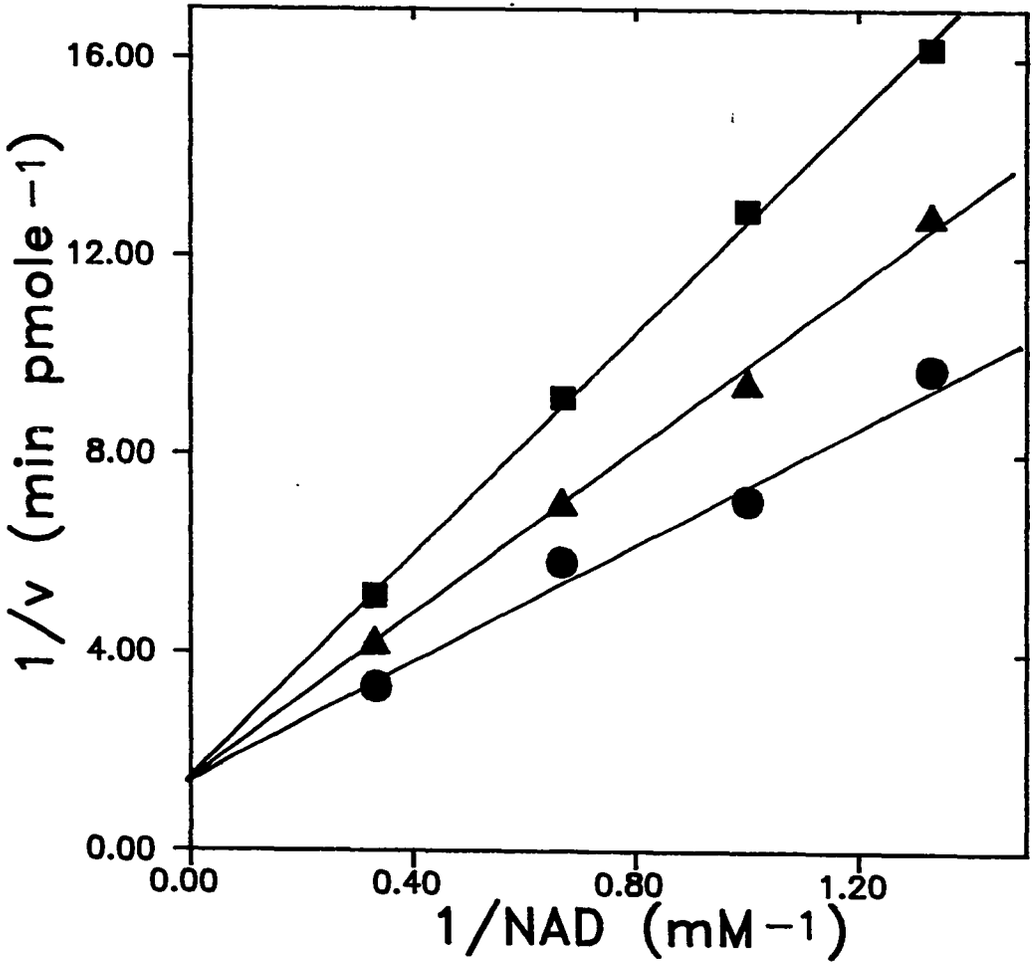
16.00
12.00
8.00
4.00
0.00
1/v (min pmole−1)
0.00
0.40
0.80
1.20
1/NAD (mM−1)

Figure 23. Double reciprocal plot of initial velocity versus NAD concentration at constant 3-aminobenzamide concentrations using the muscle transferase. The reciprocal of the initial velocities at various constant levels of 3-aminobenzamide were plotted as a function of the reciprocal of NAD concentration. The incubation mixture contained 5 ug/ml of muscle transferase (Con A fraction), 50 mM potassium phosphate pH 7.0, 0.5 mM LAME, and NAD. The concentrations of 3-aminobenzamide were: ● 0 mM, ▲ 2.5 mM, ■ 5.0 mM, ★ 7.5 mM

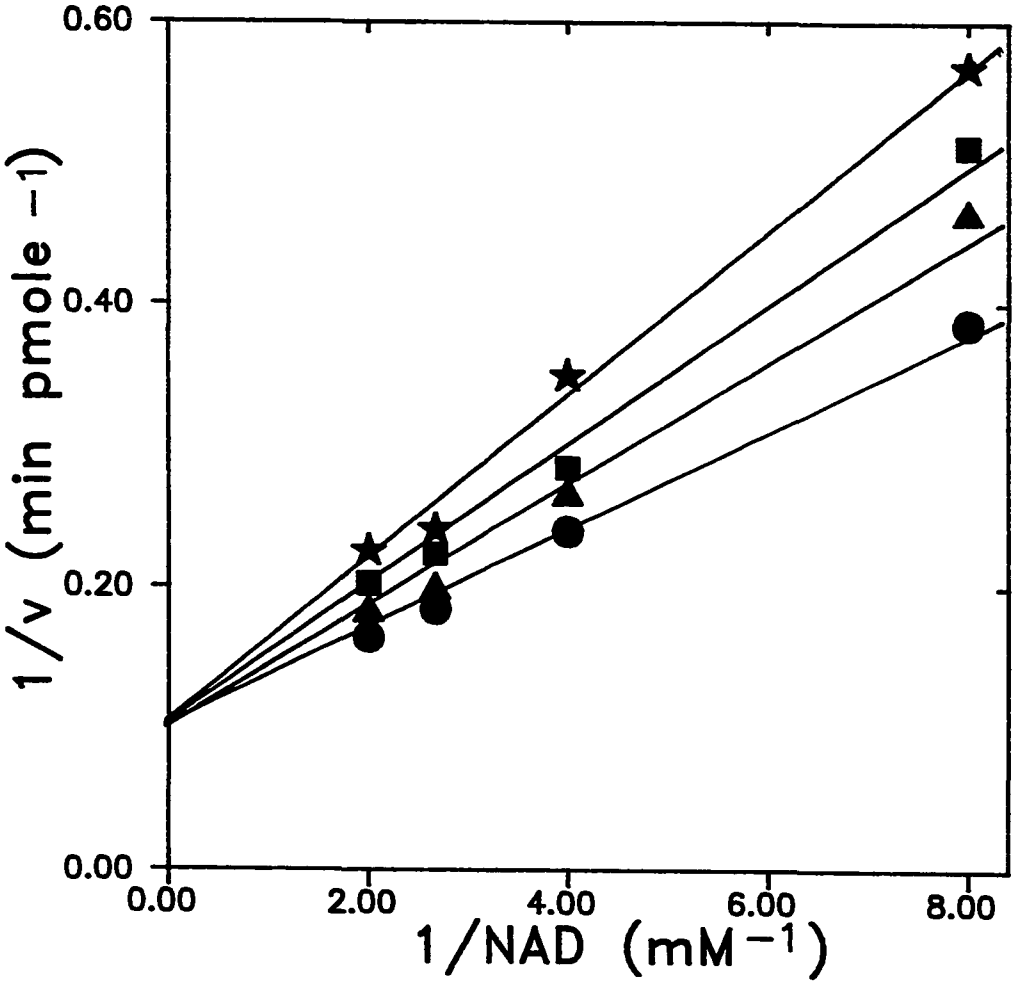
0.60
0.40
0.20
0.00
1/v (min pmole −1)
0.00
2.00
4.00
6.00
8.00
1/NAD (mM −1)

described when the lines resulting from increased inhibitor concentration converge to a single point which is not on the 1/v axis. Figures 24 and 25 show that cholera toxin and rabbit skeletal muscle enzyme exhibited this noncompetitive behavior, when incubated under the previously described conditions.

The search for a competitive inhibitor against the acceptor substrate, LAME, was not as straightforward. In order for meaningful results to be obtained the double reciprocal plots for increased inhibitor concentration must be linear. As shown in Figure 26, when an alternate substrate was chosen the double reciprocal plots were not linear. The task of finding a competitive inhibitor which was not also a substrate proved to be rather formidable. It seemed that any compound which contained the guanidino side chain was ADP-ribosylated. However, after testing a number of guanidino derivatives and searching many specialty chemical catalogs, a compound called N^G-monomethylarginine was found to be distributed by Calbiochem (San Diego, CA). This compound seemed to have all the right properties to serve as a competitive inhibitor against the acceptor substrate. It contained the guanidino side chain which was required for transferase recognition but the active site was blocked with a methyl group so it should not have been a substrate. The arginine derivative was tested and indeed was found not to be a substrate for the cholera toxin or rabbit transferase. No product peak was observed even after prolonged incubation under the standard assay conditions, as described under Methods.

Experiments were conducted in the presence of varied amounts of LAME

Figure 24. Double reciprocal plot of initial velocity versus LAME concentration at constant 3-aminobenzamide concentrations using cholera toxin. The reciprocal of the initial velocities at various 3-aminobenzamide concentrations were plotted as a function of the reciprocal of LAME concentration. The incubation mixtures contained 25 ug/ml of activated cholera toxin, 50 mM potassium phosphate pH 7.0, 20 mM DTT, 3.0 mM NAD, and LAME. The 3-aminobenzamide concentrations were: ● 0 mM, ▲ 10 mM, ■ 20 mM

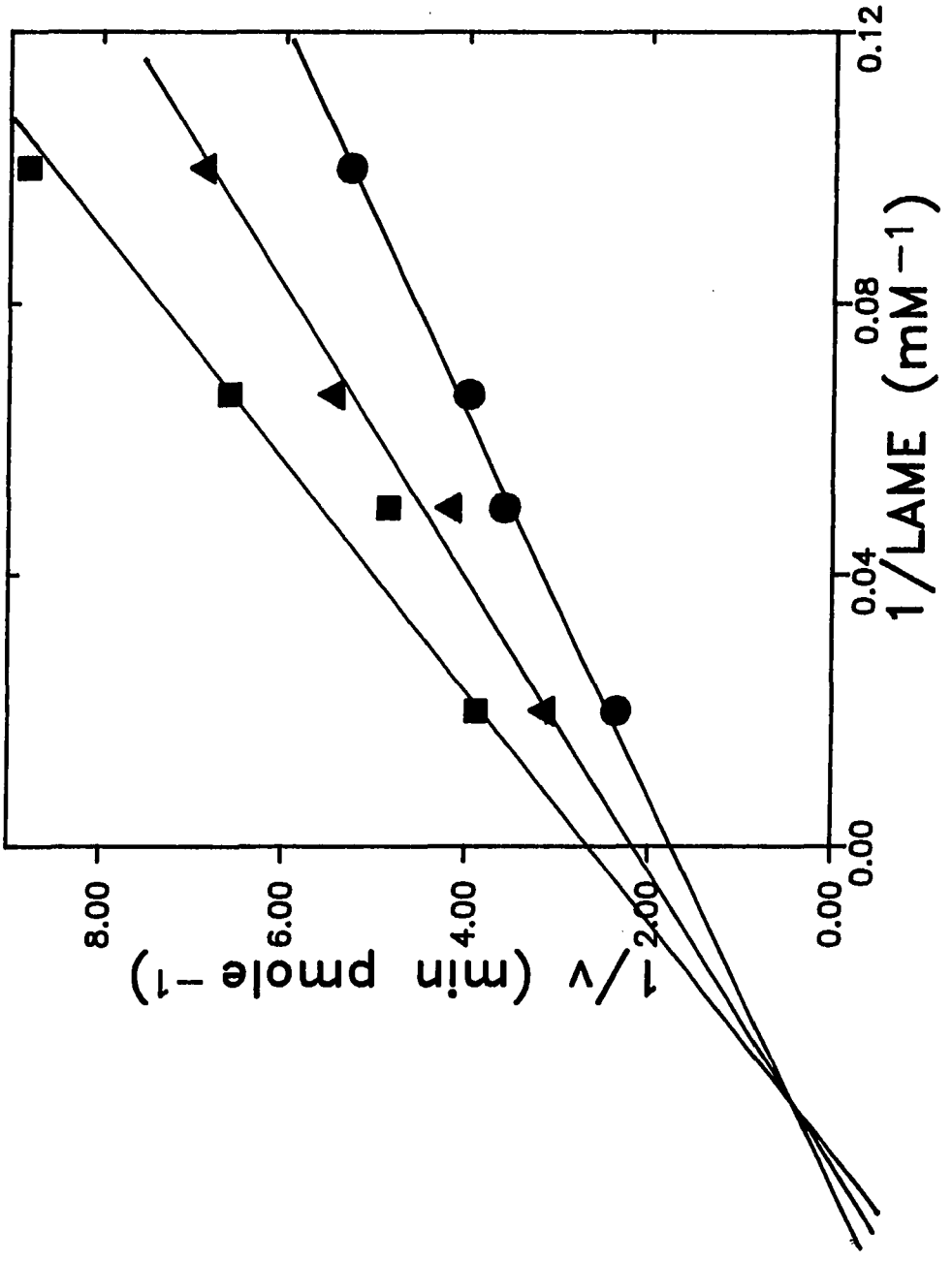
1/v (min pmole −1)
8.00
6.00
4.00
2.00
0.00
0.00
0.04
0.08
0.12
1/LAME (mM−1)

Figure 25. Double reciprocal plot of initial velocity versus LAME concentration at constant 3-aminobenzamide concentrations using the muscle transferase. The reciprocal of the initial velocities at various constant concentrations of 3-aminobenzamide were plotted as a function of LAME concentration. The incubation mixtures contained 5 ug/ml muscle transferase (Con A fraction), 50 mM potassium phosphate pH 7.0, 0.25 mM NAD, and LAME. The concentrations of 3-aminobenzamide were: ● 0 mM, ▲ 2.5 mM, ■ 5.0 mM, ★ 7.5 mM

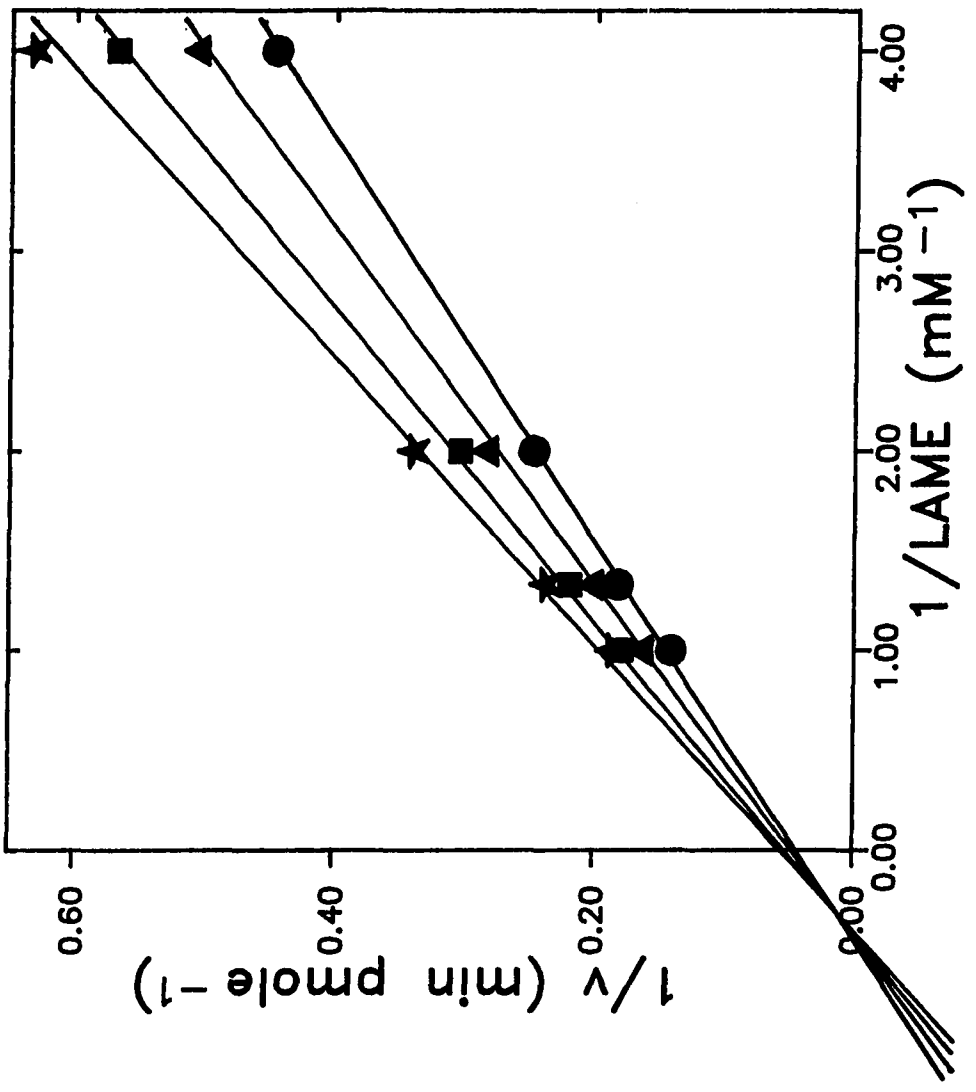
1/v (min pmole −1)
0.00
0.20
0.40
0.60
1/LAME (mM −1)
0.00
1.00
2.00
3.00
4.00

Figure 26. Double reciprocal plot of initial velocity versus NAD concentration at constant DEA-BAG concentrations using cholera toxin. The reciprocal of the initial velocities at various constant levels of DEA-BAG were plotted as a function of the reciprocal of NAD concentration. The incubation mixture contained 25 ug/ml of activated cholera toxin, 50 mM potassium phosphate pH 7.0, 20 mM DTT, 20 mM LAME, and NAD. The DEA-BAG concentrations were:

● 0 mM, ▲ 0.5 mM, ■ 1.0 mM, ★ 2.0 mM

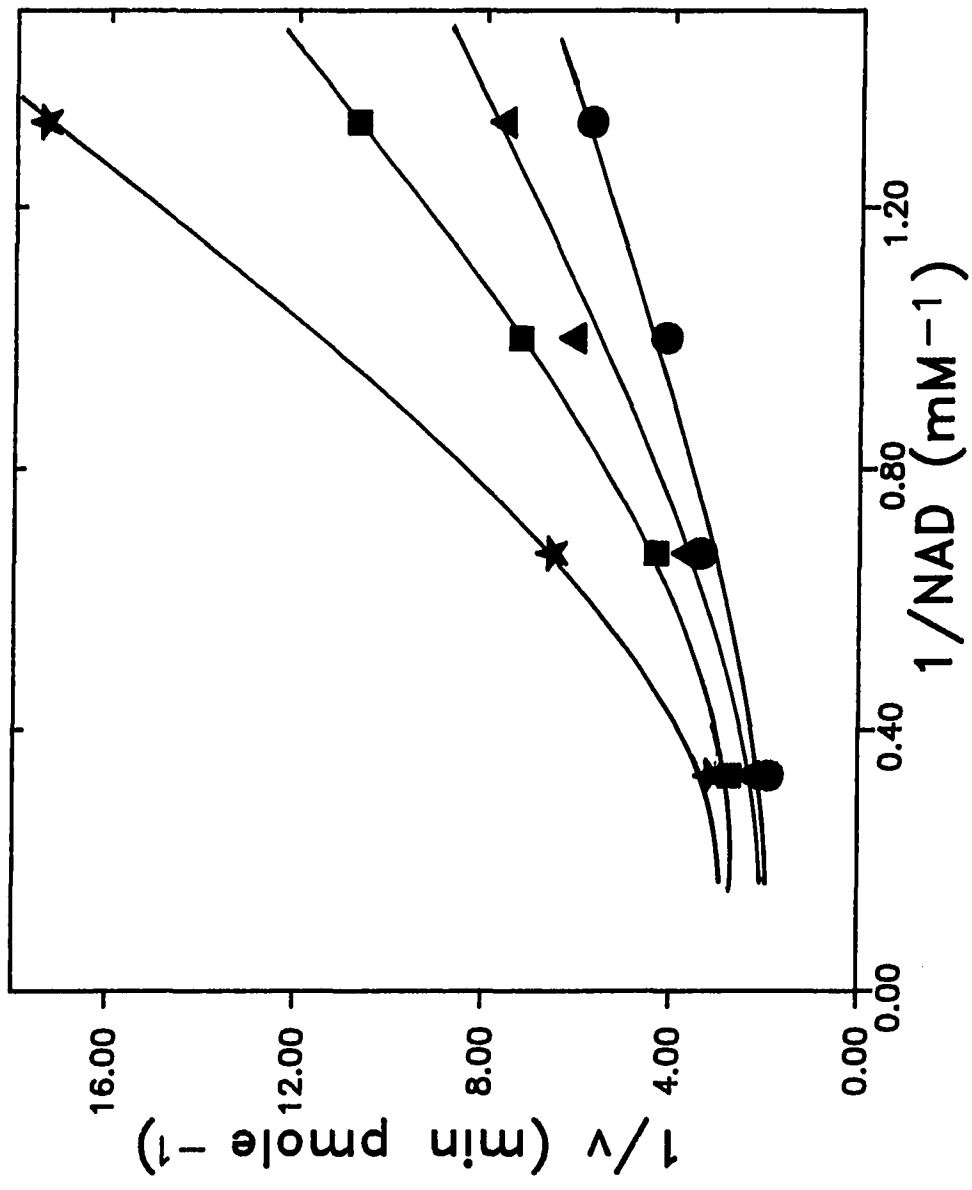
1/v (min pmole −1)
16.00
12.00
8.00
4.00
0.00
0.00
0.40
0.80
1.20
1/NAD (mM−1)

at constant levels of NAD while increasing the N^G-monomethylarginine concentration. The double reciprocal plots obtained for both enzymes revealed competitive inhibition toward LAME, as shown in Figures 27 and 28, for cholera toxin and skeletal muscle transferase, respectively. Values of 216 mM and 55 mm were calculated for the K_I of N^G-monomethylarginine using cholera toxin and rabbit skeletal muscle transferase, respectively. When the inhibitor was tested against NAD while holding the amount of LAME constant, the results indicated noncompetitive inhibition for cholera toxin, as shown in Figure 29, and the skeletal muscle transferase, as shown in Figure 30. Fromm has developed a scheme for which the type of mechanism may be determined by comparing the inhibition patterns against the two different substrates (64). This pattern of competitive-noncompetitive inhibition, which was demonstrated for both of the inhibitors, is representative of a random mechanism. Whereas, an ordered mechanism would have resulted in one of the inhibition patterns to be uncompetitive rather than noncompetitive. Refer to Figure 20 for an illustration of the random sequential mechanism which has been determined to represent the two arginine specific ADP-ribosyl transferases included in this study.

D. Specificity Studies Using Alternative Substrates

In the final phase of this study we evaluated the effect of different ADP-ribose acceptors on the K_m and V_{max} of the cholera toxin reaction. Several different amino acid derivatives, which differed by strategically located substitutions on the side chain or the

Figure 27. Double reciprocal plot of initial velocity versus LAME concentration at constant concentrations of N^G-monomethylarginine using cholera toxin. The reciprocal of the initial velocities at various constant levels of N^G-monomethylarginine were plotted as a function of the reciprocal of LAME concentration. The incubation mixtures contained 25 ug/ml of activated cholera toxin, 50 mM potassium phosphate pH 7.0, 20 mM DTT, 3.0 mM NAD, and LAME. The N^G-monomethylarginine concentrations were: ● 0 mM, ▲ 100 mM ■ 300 mM, ★ 400 mM

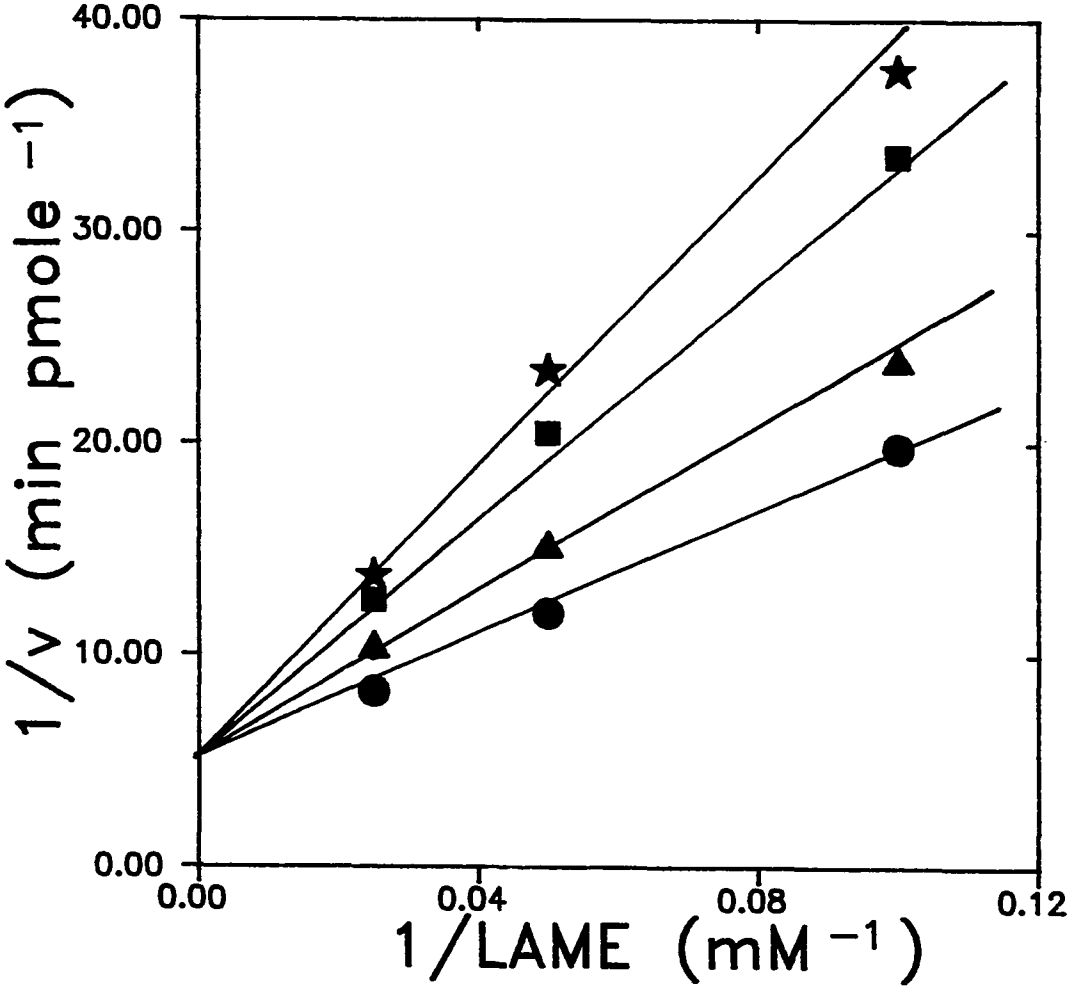
40.00
30.00
20.00
10.00
0.00
1/v (min pmole $^{-1}$)
0.00
0.04
0.08
0.12
1/LAME (mM $^{-1}$)

Figure 28. Double reciprocal plot of initial velocity versus LAME concentration at constant concentrations of N^G-monomethylarginine using the muscle transferase. The reciprocal of the initial velocities at various constant levels of N^G-monomethylarginine were plotted as a function of the reciprocal of LAME concentration. The incubation mixtures contained 5 ug/ml of muscle transferase (Con A fraction), 50 mM potassium phosphate pH 7.0, 0.25 mM NAD, and LAME. The N^G-monomethylarginine concentrations were:

● 0 mM, ▲ 10 mM, ■ 20 mM, ★ 40 mM

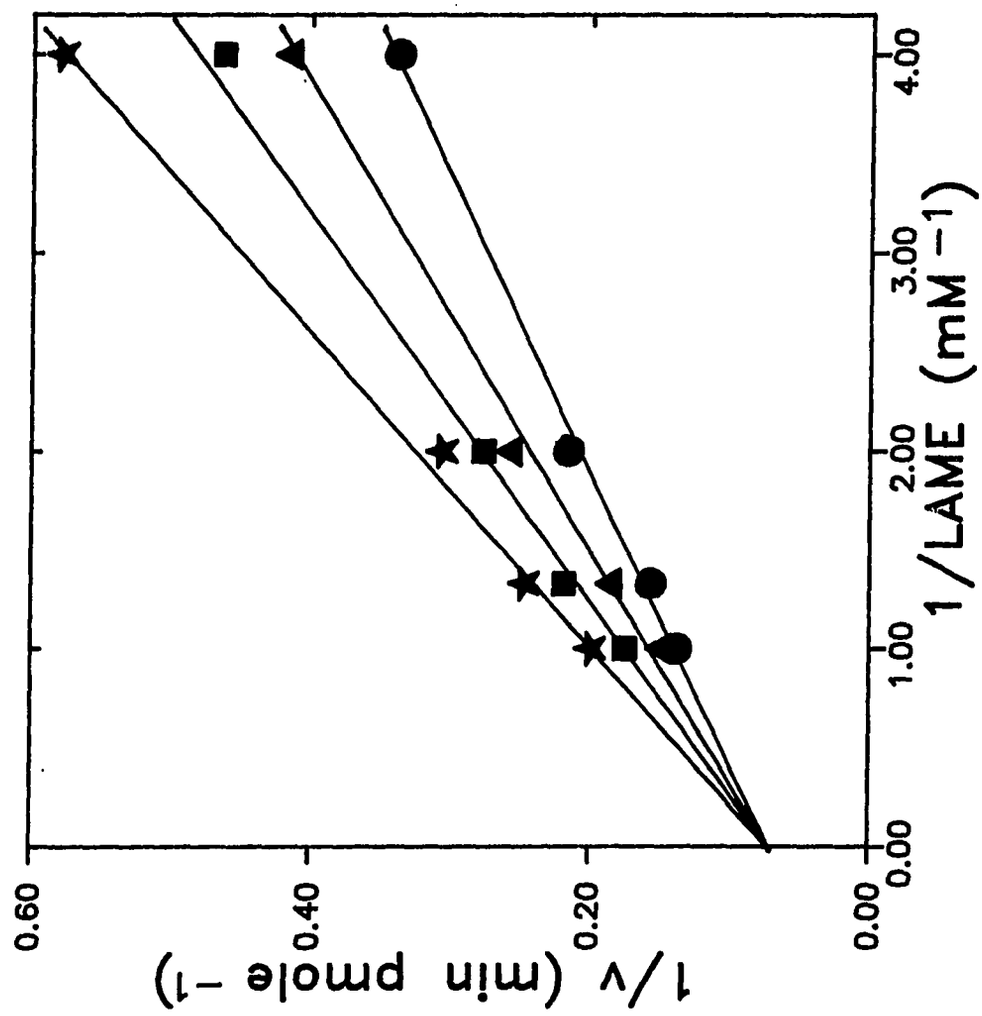
1/v (min pmole −1)
0.00
0.20
0.40
0.60
0.00
1.00
2.00
3.00
4.00
1/LAME (mM−1)

Figure 29. Double reciprocal plot of initial velocity versus NAD concentration at constant concentrations of N^G-monomethylarginine using cholera toxin. The reciprocal of the initial velocities at various constant concentrations of N^G-monomethylarginine were plotted versus the reciprocal of NAD concentration. The incubation mixtures contained 25 ug/ml of activated cholera toxin, 50 mM potassium phosphate pH 7.0, 20 mM DTT, 10 mM LAME, and NAD. The concentrations of N^G-monomethylarginine were: ● 0 mM, ▲ 100 mM, ■ 200 mM, ★ 400 mM

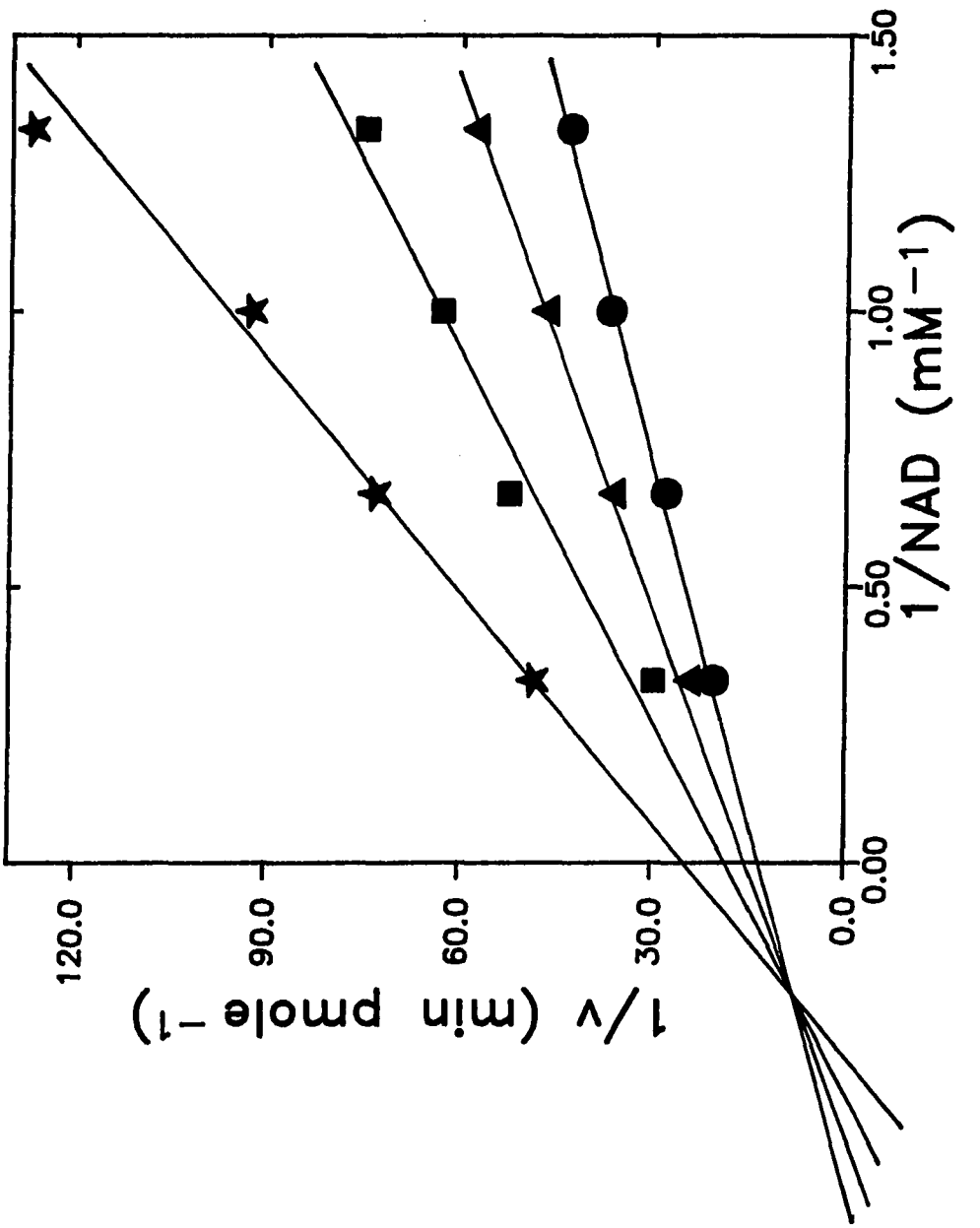
1/v (min pmole⁻¹)
120.0
90.0
60.0
30.0
0.0
0.00
0.50
1.00
1.50
1/NAD (mM⁻¹)

Figure 30. Double reciprocal plot of initial velocity versus NAD concentration at constant concentrations of N^G-monomethylarginine using muscle transferase. The reciprocal of the initial velocities at various constant concentrations of N^G-monomethylarginine were plotted as a function of the reciprocal of NAD concentration. The incubation mixtures contained 5 ug/ml of muscle transferase (Con A fraction), 50 mM potassium phosphate pH 7.0, 0.5 mM LAME, and NAD. The concentrations of N^G-monomethylarginine were: ● 0 mM, ▲ 10 mM, ■ 20 mM, ★ 40 mM

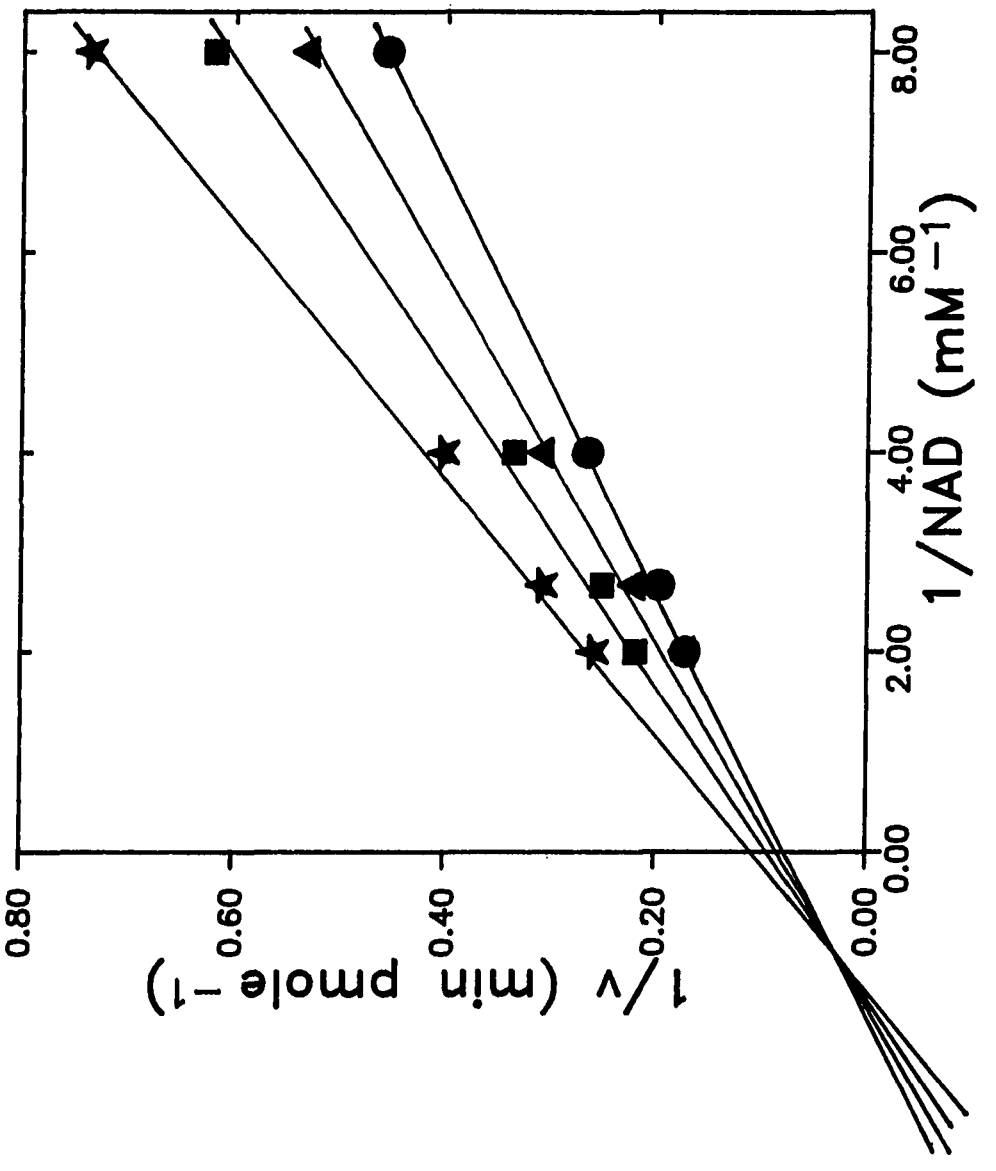
1/v (min pmole −1)
0.80
0.60
0.40
0.20
0.00
0.00
2.00
4.00
6.00
8.00
1/NAD (mM −1)

carboxylate terminal were studied. These included arginine, arginine methyl ester, canavanine, citrulline, and ornithine, whose structures are compared in Figure 31. Moss and Vaughan (15) had reported a K_m value for arginine of 75 mM with cholera toxin. This resulted in a V_{max} of 140 nmole min^{-1} mg^{-1}. We have determined the K_m for arginine methyl ester to be 39 mM, with a V_{max} of 500 nmole min^{-1} mg^{-1}. The only difference between these two substrates is that the carboxylate group on LAME is blocked with a methyl ester. This seems to be a somewhat advantageous substitution as reflected in the lower K_m and higher V_{max} of LAME versus those of arginine.

Figures 32 and 33 show the Lineweaver-Burk plots obtained from the kinetic studies which utilized canavanine as the ADP-ribose acceptor. A sequential mechanism is represented by the convergence of the lines to a single common point in the lower left quadrant for both plots. The resultant K_m value for canavanine was 17 mM with a V_{max} of 51 nmole min^{-1} mg^{-1}.

Although the substrates tested thus far are only models for the actual cellular target of cholera toxin, they clearly show that the enzyme possesses a highly specific catalytic site. The natural target for ADP-ribosylation is presumably part of a polypeptide chain where the amino and carboxyl terminals participate in amide linkages and therefore, are not charged. This specificity was reflected in the nearly ten fold increase of the K_m/V_{max} for arginine over that of LAME. Previous studies have suggested that the modified amino acid contains a guanidino side chain, such as arginine. This was supported by the experiments with

Figure 31. Comparison of arginine derivatives. K_m and V_{max} values are for cholera toxin

ARGININE

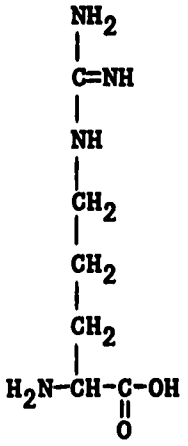

K_m = 75 mM
V_{max} = 140 $\frac{\text{nmole}}{\text{min mg}}$

ARGININE METHYL ESTER (LAME)

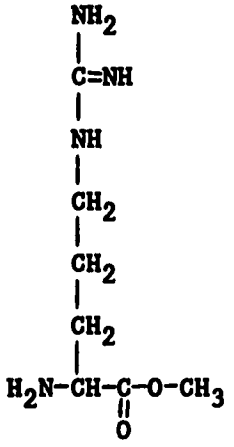

K_m = 39 mM
V_{max} = 500 $\frac{\text{nmole}}{\text{min mg}}$

CANAVANINE

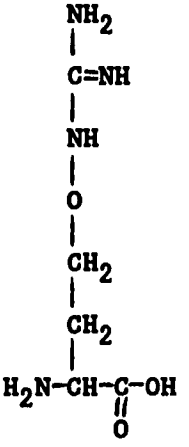

K_m = 17 mM
V_{max} = 51 $\frac{\text{nmole}}{\text{min mg}}$

CITRULLINE

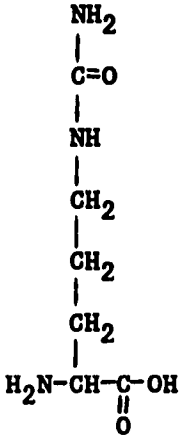

NOT A SUBSTRATE
NOT AN INHIBITOR

ORNITHINE

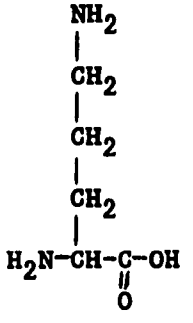

NOT A SUBSTRATE
NOT AN INHIBITOR

Figure 32. Double reciprocal plot of initial velocity versus canavanine concentrations at constant NAD concentrations using cholera toxin. The reciprocal of the initial velocities at various constant concentrations of NAD were plotted as a function of the reciprocal of canavanine concentration. The incubation mixtures contained 25 ug/ml of activated cholera toxin, 50 mM potassium phosphate pH 7.0, 20 mM DTT, and canavanine. The NAD concentrations were: ★ 1.0 mM, ▲ 1.5 mM, ● 2.0 mM, ■ 5.0 mM

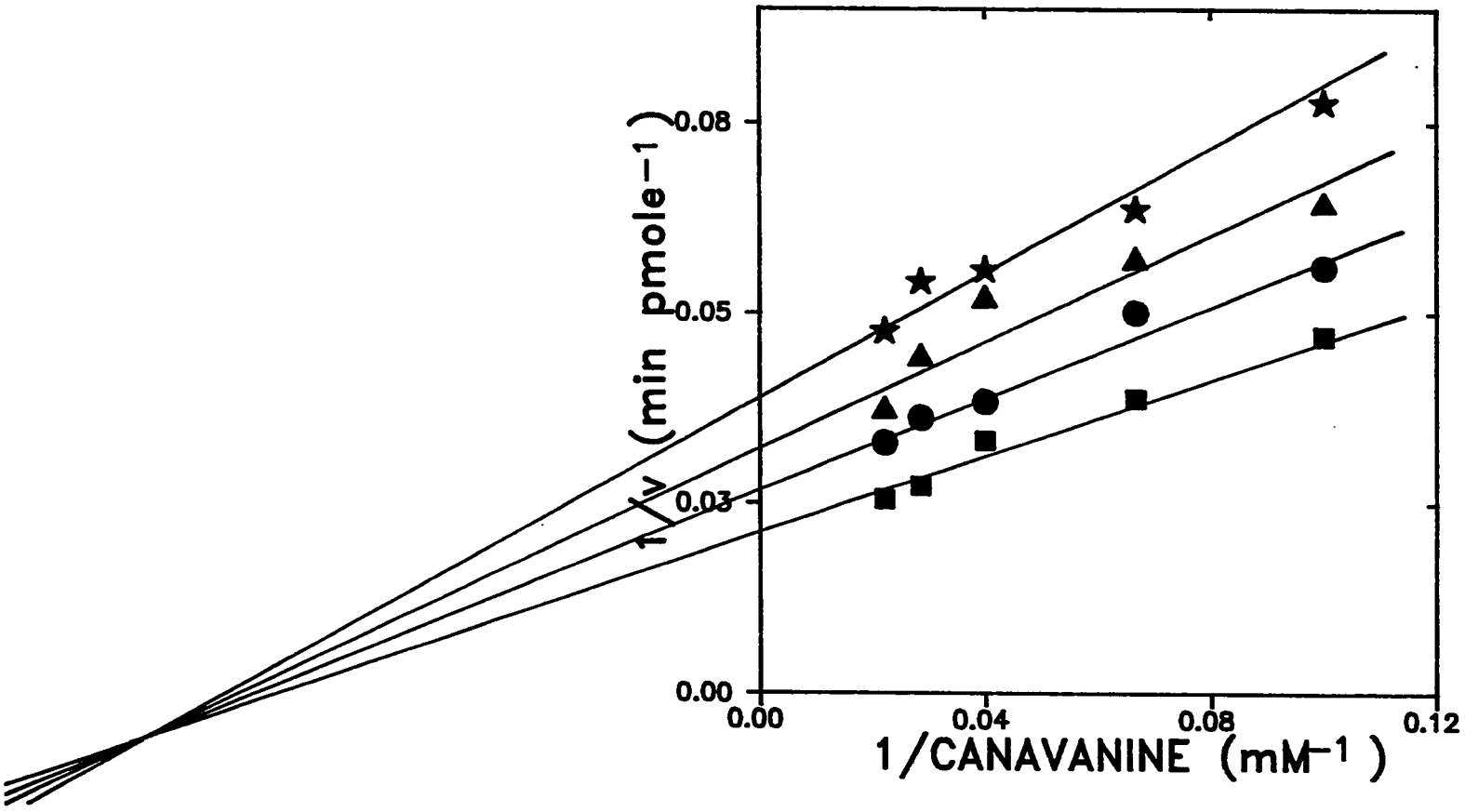
0.08
0.05
0.03
0.00
1/v (min pmole-1)
0.00
0.04
0.08
0.12
1/CANAVANINE (mM-1)

Figure 33. Double reciprocal plots of initial velocity versus NAD concentration at constant concentrations of canavanine using cholera toxin. The reciprocal of the initial velocities at various constant levels of canavanine were plotted as a function of the reciprocal of NAD concentration. The incubation mixtures contained 25 ug/ml of activated cholera toxin, 50 mM potassium phosphate pH 7.0, 20 mM DTT, and NAD. The canavanine concentrations were: ■ 10 mM, ▲ 25 mM, ● 45 mM

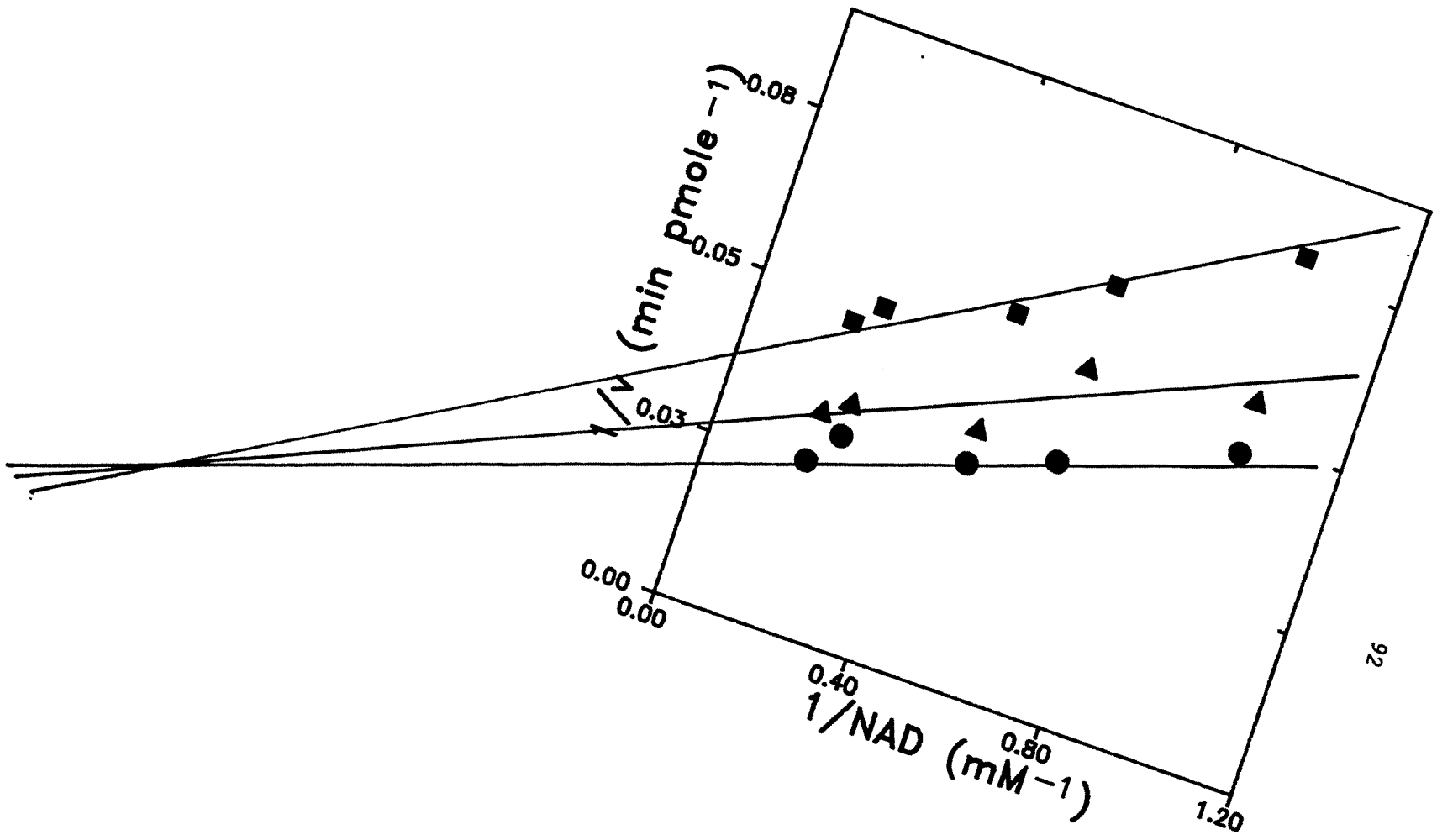
1/V (min pmole −1)
0.08
0.05
0.03
0.00
0.00
0.40
0.80
1.20
1/NAD (mM−1)

basic amino acids such as ornithine and lysine (15), which do not contain the guanidino side chain and did not serve as ADP-ribose acceptors.

Assays were also performed using citrulline, which contains a ureido rather than a guanidino moiety, as a possible ADP-ribose acceptor. This compound did not prove to be an acceptable substrate for the transferase reaction as no product peak was observed even after extensive incubation with cholera toxin and NAD. Both citrulline and ornithine were also tested for competitive inhibition against LAME, but neither one demonstrated any inhibition of the transferase activity even at very low concentrations of LAME. These results tell us that the enzyme has a very stringent arginine recognition site.

The final comparison was made between canavanine and arginine. Canavanine, like arginine, does not have the carboxyl group blocked which resulted in a characteristically low V_{max}. However, the gamma methylene group has been replaced by an oxygen which decreases the pK_a of the guanidium group to 7 versus 12.5 for arginine (67). At pH 7, the guanidium group on canavanine is only partially charged, whereas the side chain of arginine is protonated. The net effect of this substitution is that canavanine has an even greater binding affinity toward cholera toxin, which is reflected in the lower K_m value of 17 mM. This phenomenon of decreased K_m with decreased pK_a of the substrate has recently been reported for glutathione derivatives with glutathione S-transferase (68). It has been suggested that an enzyme may utilize part of the intrinsic binding energy to deprotonate a substrate. Therefore,

a substrate which is already deprotonated would bind more readily than one which carried a proton which would result in a lower K_m value. Our observations with canavanine support this hypothesis.

V. CONCLUSIONS

A. Summary

This work has described the development of an assay for arginine specific ADP-ribosyl transferases and its use in determining their kinetic mechanisms. Following is a summary of the results of this study.

1. The assay does not require a specially synthesized substrate or the use of radiolabels. L-arginine methyl ester was used as the ADP-ribose acceptor substrate because it was commercially available and cost effective. Derivatization with an OPA/2-mercaptoethanol reagent, separation by HPLC, and fluorescence detection were chosen because of their high sensitivity, selectivity, and low background noise. A limit of detection of 300 femtomoles was achieved, which proved to be more than sufficient for our studies.

2. Furthermore, the assay proved to be very flexible and reliable. The various fractions obtained during the purification of the endogenous transferase which contained detergents, exogenous proteins, and other possible contaminants were assayed without any problems or interferences. The use of gradient elution allowed for rapid sample throughput and eliminated the possibility of interferences in subsequent injections due to late eluting peaks.

3. The assay was used to determine the kinetic parameters of cholera toxin and a transferase from rabbit skeletal muscle. Initial rate studies were conducted at varying concentrations of one substrate and various fixed concentrations of the second substrate. The resulting

Lineweaver-Burk plots were representative of a sequential mechanism for both cholera toxin and the rabbit skeletal muscle transferase. This result was in agreement with previous reports of a sequential mechanism for cholera toxin and a transferase from turkey erythrocytes.

4. Kinetic parameters were determined from secondary plots of the double reciprocal plots and compared with those calculated by a computer modeling program. The K_m values of 5.6 mM and 39 mM for NAD and LAME, respectively, for cholera toxin were in close agreement with previously reported values. Kinetic parameters for the rabbit skeletal muscle transferase also were determined. However, these were found to be quite different from those reported for the avian transferase. The K_m value of 0.56 mM for NAD is 80 fold higher than that reported for the avian enzyme. But, the K_m value for LAME of 1.2 mM was only 6 fold greater than the avian transferase. This difference was attributed to the fact that the rabbit transferase was purified from a membrane fraction whereas the turkey transferase originated from the soluble fraction. It is concluded that there is an intrinsic difference in cellular function and specificity for each enzyme which is reflected in the different K_m values. However, the V_{max} values of 40 umole min^{-1} mg^{-1} for the muscle transferase and 31 umoles min^{-1} mg^{-1} for the erythrocyte transferase are exceptionally close.

5. Inhibition studies were conducted, with both cholera toxin and the rabbit muscle transferase to determine if the sequential mechanisms were random or ordered. Competitive inhibitors, which were not substrates, were found for both NAD and LAME. The compound

3-aminobenzamide was found to be competitive against NAD with a K_I of 35 mM for cholera toxin and 14 mM for the rabbit muscle transferase. It was also determined to be noncompetitive against LAME for both enzymes. The compound N^G-monomethylarginine was found to be competitive against LAME with a K_I of 216 mM and 55 mM for cholera toxin and the muscle enzyme, respectively. As with the 3-aminobenzamide, this inhibitor was found to be noncompetitive against the second substrate with both enzymes. This pattern of competitive-noncompetitive inhibition demonstrated by both inhibitors is indicative of a random mechanism. Results from the initial rate studies combined with those from the inhibitor studies allowed us to conclude that both enzymes follow a random sequential kinetic mechanism.

6. Finally, specificity studies were conducted using cholera toxin with various substrates which were closely related to arginine but contained significant modifications. Compounds which did not contain the guanidino side chain such as citrulline, lysine, and ornithine were not recognized as substrates by the enzyme and did not inhibit the transferase activity. These results demonstrated the absolute requirement of the guanidinium group for substrate recognition. The increased K_m/V_{max} for arginine over LAME was attributed to the charged carboxylate group which would not be present in the endogenous substrate. Canavanine had a relatively low K_m of 17 mM which suggested that the substrate must undergo deprotonation prior to the catalytic reaction.

Although small molecular weight compounds are only models for the endogenous substrate, the results clearly show that the enzyme possesses a catalytic site which is highly specific for the substrate.

B. Suggestions for Future Work

This work has given us some insight as to the way arginine specific ADP-ribosyl transferases carry out their catalytic activity. But, the most ominous question still remains unanswered: what are the functions of the transferases *in vivo*? Many experiments will have to be performed to answer this question, not the least of which will be to determine the identity of the endogenous substrate(s). Once the substrates have been identified, the role of ADP-ribosyl transferases in the regulation of cellular metabolism may be established.

It also will be interesting to learn the similarities and differences between the different types of endogenous transferases. There is currently no good assay for cysteine specific ADP-ribosyl transferases. We have performed initial experiments using fluorescent cysteine and cystine derivatives as possible substrates but have been unable to observe a reaction with pertussis toxin. The development of an assay cocktail which contains substrates for both the arginine and cysteine specific transferases would be a useful tool in screening various tissues for these activities.

VI. LITERATURE CITED

1. Nishizuka, Y.; Ueda, K.; Honjo, T.; Hayaishi, O. J. Biol. Chem. 1968, 243, 3765-3767.
2. Hayaishi, O.; Veda, K., Eds., ADP-ribosylation reactions: Biology and Medicine; Academic Press: New York, 1982.
3. Miwa, M.; Sugimura, T. J. Biol. Chem. 1971, 246, 6362-6364.
4. Miwa, M.; Ishihara, M.; Takishima, S.; Takasuka, N.; Maeda, M.; Yamaizumi, A.; Sugimara, T. J. Biol. Chem. 1981, 256, 2916-2921.
5. Benjamin, R.C.; Gill, D.M. J. Supramol. Struct. Suppl. 1978, 2, 74.
6. Caplan, A. I.; Rosenberg, M. J. Proc. Natl. Acad. Sci., USA 1975, 72, 1852-1857.
7. Claycomb, W. C. FEBS Lett. 1976, 61, 231-233.
8. Ghani, Q.P.; Hollenberg, M. Biochem. Biophys. Res. Commun. 1978, 81, 886-891.
9. Farzanch, F.; Pearson, C. K. Biochem. Biophys. Res. Commun. 1978, 84, 537-543.
10. Miwa, M.; Oda, K.; Segawa, K.; Tanaka, M.; Irie, S.; Yamaguchi, N.; Kuchino, T.; Shiroki, K.; Shimojo, H.; Sakura, H.; Matsuhima, T.; Sugimara, T. Arch. Biochem. Biophys. 1977, 181, 313-321.
11. Chambon, P.; Weill, J. D.; Doly, J.; Strosse, M. T.; Mandell, P. Biochem. Biophys. Res. Commun. 1966, 25, 638-643.
12. Jacobson, M. K.; Levi, V.; Juarez-Salinas, H.; Barton, R. A.; Jacobson, E. L. Cancer Res. 1980, 40, 1797-1802.

13. Smulson, M. E.; Stark, P.; Gazzoli, M.; Roberts, J. H. Exp. Cell. Res. 1975, 90, 175-182.

14. Whish, W. J. D.; Davies, M. I.; Shall, S. Biochem. Biophys. Res. Commun. 1975, 65, 722-730.

15. Moss, J.; Vaughan, M. J. Biol. Chem. 1977, 252, 2455-2457.

16. Moss, J.; Manganiello, V. C.; Vaughan, M. Proc. Natl. Acad. Sci., USA 1976, 73, 4424-4427.

17. Moss, J.; Richardson, S. H. J. Clin. Invest. 1978, 62, 281-285.

18. Honjo, T.; Nishizuka, Y.; Hayaishi, O.; Kato, I. J. Biol. Chem. 1968, 243, 3553-3555.

19. Katada, T.; Ui, M. Proc. Natl. Acad. Sci., USA 1982, 79, 3129-3133.

20. Brightwell, M. D.; Leech, C. E.; O'Farrell, M. K.; Whish, W. J. D.; Shall, S. Biochem. J. 1975, 147, 119-129.

21. Moss, J.; Stanley, S. J.; Watkins, P. A. J. Biol. Chem. 1980, 255, 5838-5840.

22. Moss, J.; Stanley, S. J. Proc. Natl. Acad. Sci., USA 1981, 78, 4809-4812.

23. Moss, J.; Stanley, S. J. J. Biol. Chem. 1981, 256, 7830-7833.

24. Tanigawa, Y.; Tsuchiya, M.; Imai, Y.; Shimoyama, M. J. Biol. Chem. 1984, 259, 2022-2029.

25. Godeau, F.; Belin, D.; Koide, S. S. Anal. Biohem. 1984, 137, 287-296.

26. Hammerman, M. R.; Hanson, V. A.; Morrissey, J. J. J. Biol. Chem. 1982, 257, 12380-12386.

27. DeWolf, M. J. S.; Vitti, P.; Ambesi-Impiombato, F. S.; Kohn, L. D. J. Biol. Chem. 1981, 256, 12287-12296.

28. Soman, G.; Mickelson, J. R.; Louis, C.F.; Graves, D. J. Biochem. Biophys. Res. Commun. 1984, 120, 973-980.

29. Peterson, J. E.; Larew, J. S. A.; Graves, D. J., submitted for publication in J. Biol. Chem.

30. Kharadia, S. V.; Graves, D. J. J. Biol. Chem. 1987, 262, 17379-17383.

31. Tanigawa, Y.; Tsuchiya, M.; Imai, Y.; Shimoyama, M. FEBS Lett. 1983, 160, 217-220.

32. Filetti, S.; Rapport, B. J. Clin. Invest. 1981, 68, 461-467.

33. Reilly, T. M.; Beckner, S.; McHugh, E. M.; Blecher, M. Biochem. Biophys. Res. Commun. 1981, 113, 135-141.

34. Richter, C.; Winterhalter, K. H.; Baumhuter, S.; Lotscher, H. R.; Moser, B. Proc. Natl. Acad. Sci., USA 1983, 80, 3188-3192.

35. Moss, J.; Jacobson, M. K.; Stanley, S. J. Proc. Natl. Acad. Sci., USA 1985, 82, 5603-5607.

36. Moss, J.; Oppenheimer, N. J.; West, R. E. C., Jr.; Stanley, S. J. Biochem. 1986, 25, 5408-5414.

37. Sari, L. L.; Pope, M. R.; Merrell, S. A.; Ludden, P. W. J. Biol. Chem. 1986, 261, 4973-4977.

38. Chang, Y. C.; Soman, G.; Graves, D. J. Biochem. Biophys. Res. Commun. 1986, 139, 932-939.

39. Kim, E. S.; Graves, D. J., submitted for publication in J. Biol. Chem.

40. West, R. E. C., Jr.; Moss, J.; Vaughan, M.; Liu, T.; Liu, T. Y. J. Biol. Chem. 1985, 260, 14428-14430.

41. Chang, F. H.; Bourne, H. R. J. Biol. Chem. 1989, 264, 5352-5357.

42. Watkins, P. A.; Moss, J.; Vaughan, M. J. Biol. Chem. 1980, 255, 3959-3963.

43. Mekalanos, J. J.; Collier, R. J.; Romig, W. R. J. Biol. Chem. 1979, 254, 5849-5854.

44. Soman, G.; Tomer, K. B.; Graves, D. J. Anal. Biochem. 1983, 134, 101-110.

45. Soman, G.; Narayanan, J.; Martin, B. L.; Graves, D. J. Biochem. 1986, 25, 4113-4119.

46. Narayanan, J., M.S. thesis, Iowa State University, 1988.

47. Cori, G. T.; Slein, M. W.; Cori, C. F. J. Biol. Chem. 1948, 173, 605-618.

48. Kornberg, A. J. Biol. Chem. 1950, 182, 805-813.

49. Storer, A. C.; Cornish-Bowden, A. Biochem. 1974, 141, 205-209.

50. Product Bulletein #PB-47, Dynamax-TI Titanium Columns; Rainin Instrument Co., Inc.; Woburn, MA, 1989.

51. Product Literature, Dionex BioLC Series; Dionex Corp.; Sunnyvale, CA, 1987.

52. Rossomando, E. F. High Performance Liquid Chromatography in Enzymatic Analysis; John Wiley & Sons: New York, 1987.

53. Sloan, D. L. Adv. in Chrom. 1984, 23, 97-125.

54. Skoog, D. A. Principles of Instrumental Analysis, 3rd ed.; Saunders College Publishing: Philadelphia, 1985; p 793.

55. Rossomando, E. F. LC-GC 1988, 5, 880-889.

56. Roth, M. Anal. Chem. 1971, 43, 880-882.

57. Oppenheimer, N. J. J. Biol. Chem. 1978, 253, 4907-4910.

58. Moss, J.; Stanley, S. J.; Oppenheimer, N. J. J. Biol. Chem. 1979, 254, 8891-8894.

59. Galloway, T. S.; Van Heyningen, S. Biochem. J. 1987, 244, 225-230.

60. Van Heyningen, S. Bioscience Reports 1982, 2, 135-146.

61. Ribi, H. O.; Ludwig, D. S.; Mercer, K. L.; Schoolnik, G. K.; Kornberg, R. D. Science 1988, 239, 1272-1276.

62. Viola, R. "The Kinetics Program", adapted from Cleland, W. W. Meth. in Enz. 1979, 63, 103-138.

63. Osborne, J. C.; Stanley, S. J.; Moss, J. Biochem. 1985, 24, 5235-5240.

64. Fromm, H. J. Molecular Biology Biochemistry and Biophysics: Initial Rate Enzyme Kinetics; Springer-Verlag: New York, 1975; Vol. 22, pp 121-139.

65. Rankin, P. W.; Jacobson, E. L.; Benjamin, R. C.; Moss, J.; Jacobson, M. K. J. Biol. Chem. 1989, 264, 4312-4317.

66. Purnell, M. R.; Whish, W. Biochem. J. 1979, 185, 775-777.

67. Tabatabai, L. B., Ph.D. dissertation, Iowa State University, 1976.

68. Graminski, G. F.; Kubo, Y.; Armstrong, R. N. Biochem. 1989, 28, 3562-3568.

VII. ACKNOWLEDGMENTS

I would like to thank my major professor, Don Graves, for his guidance and understanding over the last 4 years. He has helped to broaden my knowledge by allowing me to expand my analytical background into the field of biochemistry. The members of his research group, both past and present, also have helped me achieve an understanding of the complexities involved in biochemical analyses. Jon Peterson deserves special thanks for allowing me to gain valuable experience by working with him on the purification project.

Especially appreciated are the many helpful discussions with Dr. Herb Fromm whose patience in explaining kinetic mechanisms was indeed a virtue.

I also would like to thank Dr. Dennis Johnson and the members of his research group for their friendship and for making me feel welcome as an adopted member of "Electrochemistry Group I".

Finally, I owe my biggest "Thank-you" to my family. My parents have stood by me for the last 27 years and always encouraged me to do my best. My daughter, Ashley, has been an inspiration and a ray of hope when everything seemed hopeless. And then there's Larry. To most of you he is my husband, but he also is my proof reader, my chief critic, my friend, and the world's best stepfather. Without him I would not be what I am today, Mrs. Dr. Larew!

It is this type of encouragement from my parents, my family, and my friends that give me the courage to keep trying and eventually succeed.

VIII. APPENDIX

The rate expression given by Equation 1 is for a Sequential mechanism as illustrated in Figure 12.

$$\frac{1}{v} = \frac{1}{V_1} + \frac{K_a}{V_1(A)} + \frac{K_b}{V_1(B)} + \frac{K_{ia}\,K_b}{V_1(A)(B)} \qquad (1)$$

Where, v is the initial velocity, V_1 is the maximal velocity in the forward direction, K_a and K_b are the Michaelis constants, and K_{ia} is the enzyme-substrate dissociation constant.

When the reciprocal of the initial velocity is plotted versus the reciprocal of substrate A concentration (Figures 10 and 14), the intercept of Equation (1) is described by

$$\text{Intercept} = \frac{1}{V_1} + \frac{K_b}{V_1(B)} \qquad (2)$$

and the slope of Equation (1) is described by

$$\text{Slope} = \frac{K_a}{V_1} + \frac{K_{ia}K_b}{V_1(B)} . \qquad (3)$$

When the reciprocal of the initial velocity is plotted versus the reciprocal concentration of the second substrate (Figure 11), substitutions of K_a for K_b and A for B are made in Equation 2 and K_b for K_a and A for B in Equation 3.

Secondary plots of intercepts and slopes versus the reciprocal of substrate concentration may then be constructed. When the intercepts are plotted versus the reciprocal of the second substrate concentration, B,

(Figures 17 and 19) the intercept of this plot is described by

$$\text{intercept} = \frac{1}{V_1} \qquad (4)$$

and the slope is described by

$$\text{slope} = \frac{K_b}{V_1} . \qquad (5)$$

Secondary plots of the slopes versus the reciprocal of the second substrate (Figures 16 and 18) are described by

$$\text{intercept} = \frac{K_a}{V_1} \qquad (6)$$

and

$$\text{slope} = \frac{K_{ia}K_b}{V_1} \qquad (7)$$

The value of V_1 may be calculated from Equation 4 and used in Equation 5 to calculate K_b, and in Equation 6 to calculate K_a. The values for K_b and V_1 may then be used in Equation 7 to calculate K_{ia}.